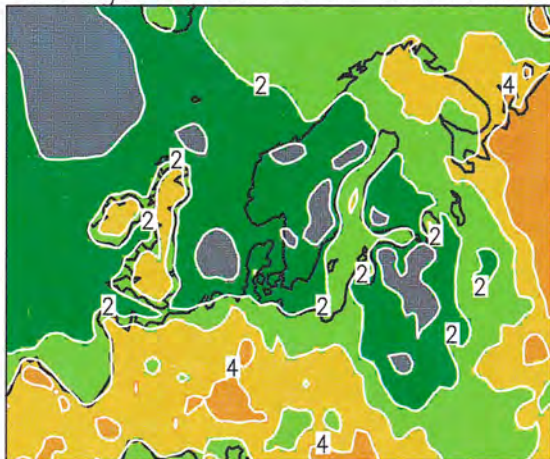
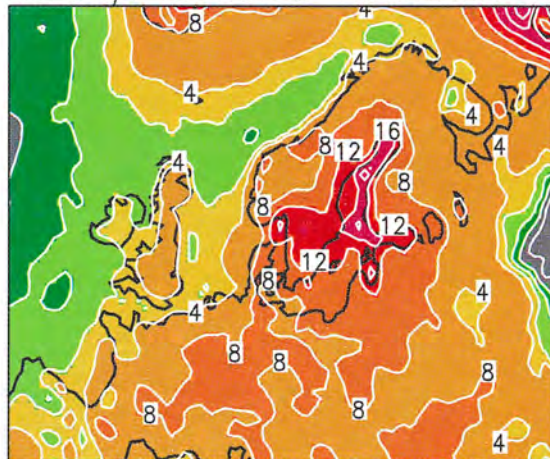


Change in summer maximum



Change in winter minimum



The First Rossby Centre Regional Climate Scenario – Dynamical Downscaling of CO₂-induced Climate Change in the HadCM2 GCM

Jouni Räisänen, Markku Rummukainen, Anders Ullerstig,
Björn Bringfelt, Ulf Hansson, and Ulrika Willén
Rossby Centre, SMHI

Cover illustration: Changes in average annual temperature extremes (the highest summer maximum temperature and the lowest winter minimum temperature), obtained as 10-year mean difference between the first Rossby Centre scenario and control runs.

**The First Rossby Centre
Regional Climate Scenario –
Dynamical Downscaling of
CO₂-induced Climate Change
in the HadCM2 GCM**

**Jouni Räisänen, Markku Rummukainen, Anders Ullerstig,
Björn Bringfelt, Ulf Hansson, and Ulrika Willén
Rossby Centre, SMHI**

Report Summary / Rapportsammanfattning

Issuing Agency/Utgivare		Report number/Publikation	
Swedish Meteorological and Hydrological Institute S-601 76 NORRKÖPING Sweden		RMK No. 85	
		Report date/Utgivningsdatum February 1999	
Author (s)/Författare Jouni Räisänen, Markku Rummukainen, Anders Ullerstig, Björn Bringfelt, Ulf Hansson and Ulrika Willén			
Title (and Subtitle/Titel) The first Rossby Centre regional climate scenario – Dynamical downscaling of CO ₂ -induced climate change in the HadCM2 GCM			
Abstract/Sammandrag <p>Results of the first 10-year climate change experiment made with the Rossby Centre regional climate model (RCA) are described. The boundary data for this experiment were derived from two simulations with the global HadCM2 ocean-atmosphere GCM, a control run and a scenario run with 150% higher equivalent CO₂ and 2.6°C higher global mean surface air temperature.</p> <p>Some of the climate changes (scenario run – control run) simulated by RCA are substantial. The annual mean temperature in the Nordic region increases by roughly 4°C, with largest warming in winter. Annual absolute minimum temperatures increase even more than the winter mean temperature, presumably due to greatly reduced snow and ice cover. Precipitation is also simulated to increase in northern Europe, locally by 40% in the annual mean in Swedish Lapland. The larger time mean precipitation is accompanied by a marked increase in the number of days with heavy precipitation.</p> <p>The large-scale temperature and precipitation changes simulated by RCA are similar to those in HadCM2. Unlike HadCM2, however, RCA simulates a strong local maximum of wintertime warming over the northern parts of the Baltic Sea. This is caused by radically reduced ice cover, but the crude treatment of the Baltic Sea and its ice even in RCA complicates the interpretation. Large differences between the models occur in the simulated changes of winter mean total cloudiness and near-surface wind speed, demonstrating the sensitivity of these to differences in resolution and/or physical parameterizations.</p> <p>The significance of the simulated climate changes against interannual variability depends on the parameter considered. Of highest statistical significance are changes in surface air temperature and strongly temperature-related variables such as snow and ice cover. In general, changes in annual means are more commonly significant than those in seasonal means. The impact of the limited averaging period is also studied by comparing the 10-year mean climate changes simulated by the driving HadCM2 model with climate changes inferred from much longer HadCM2 integrations.</p>			
Key words/sök-, nyckelord Climate change, climate scenario, regional climate modelling			
Supplementary notes/Tillägg This work is a part of the SWECLIM programme		Number of pages/Antal sidor 56	Language/Språk English
ISSN and title/ISSN och titel 0347-2116 SMHI Reports Meteorology Climatology			
Report available from/Rapporten kan köpas från: SMHI S-601 76 NORRKÖPING Sweden			

Contents

1	Introduction	1
2	Models, experimental design and control climate	2
2.1	The HadCM2 global climate model	2
2.2	RCA – the Rossby Centre regional Atmospheric climate model	3
2.3	The first two 10-year simulations.....	4
2.4	Climate in the RCA control simulation	6
2.4.1	Circulation and atmospheric temperatures	6
2.4.2	Surface air temperature.....	6
2.4.3	Precipitation and surface hydrology	7
2.4.4	Total cloudiness.....	7
2.4.5	Snow and ice cover.....	7
3	Comparison of climate changes in RCA and HadCM2	8
3.1	Atmospheric circulation	9
3.2	Surface air temperature.....	11
3.3	Precipitation.....	14
3.4	Total cloudiness	15
3.5	Mean wind speed at 10 m height.....	17
3.6	Radiation balance	19
3.7	Surface energy balance.....	22
3.8	Area mean statistics	24
4	Further aspects of climate change in RCA	30
4.1	Surface hydrology.....	30
4.2	Snow and ice.....	32
4.3	Variability of temperature and precipitation	34
5	Statistical significance of simulated climate change: a summary	39
6	Climate change in HadCM2 – comparison of the 10-year time slice with longer model runs	43
7	Summary and concluding remarks	50
	Acknowledgements	53
	References	54

1 Introduction

Rosby Centre, a new research unit in the Swedish Meteorological and Hydrological Institute (SMHI) and a part of the SWEdish regional CLimate Modelling programme (SWECLIM), has recently conducted its first set of two 10-year regional climate simulations. The model used for these experiments was modified from HIRLAM cycle 2.5 and is known as RCA – the Rosby Centre regional Atmospheric climate model. The model is described by Rummukainen et al. (1998), who also provide a basic documentation of the results in one of the two 10-year simulations. In this simulation, RCA was run with 44 km horizontal resolution driven by large-scale boundary data from a control ('present climate') run made with the global HadCM2 ocean-atmosphere general circulation model (Johns et al. 1997).

The second 10-year RCA run ('scenario run') used boundary data from a HadCM2 simulation with increased atmospheric CO₂ (Mitchell and Johns 1997). The focus of this report are the differences between the second and the first simulation, that is, the CO₂-induced climate changes in the RCA regional model. Some aspects of these were already discussed in SWECLIM (1998) with emphasis in the Nordic region, but a wider selection of results is included here. In addition, where available data from the driving HadCM2 simulations allow, climate changes in RCA are compared with those in HadCM2. This is an important point, for example, in assessing the need and value of regional climate modelling for constructing scenarios of future climate. Finally, another important issue is the relative shortness of the simulated period, only 10 model years. Like nature in reality, climate models exhibit substantial internally generated variability even without changes in external forcing conditions, and the relative importance of this variability increases with decreasing simulation period. Thus, it is necessary to ask how well the 'signal' associated with increasing CO₂ is visible against this inevitable 'noise', and how this depends on the aspect considered.

The report starts with a brief review of issues largely addressed in earlier studies. These include descriptions of the driving global HadCM2 model and the RCA regional climate model, the experimental design for the first 10-year simulations, and a summary of the main findings in the evaluation of the control run. After this (Sections 3 and 4) the simulated climate changes are discussed, including the time mean climate in the free atmosphere and near the surface, radiation fluxes and surface energy balance, and some aspects of the daily variability of surface climate. The statistical significance of the simulated climate changes is indicated in most of the maps shown in Sections 3 and 4, but the basic findings concerning this issue are summarized in Section 5. In Section 6, the impact of the limited averaging period is studied in a more concrete manner, by comparing the 10-year HadCM2 runs used to drive RCA with longer runs made with the same global model. The report ends with a summary and some concluding remarks in Section 7.

2 Models, experimental design and control climate

2.1 The HadCM2 global climate model

The Hadley Centre coupled ocean-atmosphere general circulation model (OAGCM) HadCM2 is described in some detail by Johns (1996) and Johns et al. (1997). HadCM2 is a state-of-the-art OAGCM with a horizontal resolution of 2.5° in latitude \times 3.75° in longitude, or 280×210 km at 60°N . It includes fully dynamic three-dimensional model components for both the atmosphere and the ocean, with parametrical representation for several subgridscale physical processes. Various thermodynamical and hydrological processes occurring at the land surface and the development and movement of sea ice are also modelled. Technical characteristics of the model are summarized in Table 1.

Table 1. Characteristics of the HadCM2 climate model. *SW* denotes short-wave (solar) and *LW* long-wave (terrestrial) radiation. Climate sensitivity is the equilibrium change in global mean surface air temperature due to a doubling of CO_2 .

Atmospheric resolution	$2.5^\circ\text{lat} \times 3.75^\circ\text{lon}$; 19 hybrid levels
Ocean resolution	$2.5^\circ\text{lat} \times 3.75^\circ\text{lon}$; 20 levels
Spinup	Coupled spinup for 510 years
Radiation scheme	4 bands in SW + 6 bands in LW (Slingo and Wilderspin 1986; Slingo 1989). Trace gases explicitly accounted for are H_2O , O_3 and CO_2 .
Convection parameterization	Penetrative convection scheme with explicit downdraught (Gregory and Rowntree 1990; Gregory and Allen 1991)
Vertical diffusion	First-order (Smith 1990)
Surface scheme	Soil temperature predicted in 4 layers with zero heat flux at the base. Snow cover and soil water predicted. Canopy effects are taken into account (Warrilow et al. 1986).
Time integration scheme	Split-explicit (Cullen and Davies 1991), advection with Heun (Mesinger 1981).
Time steps	30 min atmosphere; 60 min ocean
Explicit corrections during time integration	Atmospheric energy and mass loss; negative humidities
Flux corrections	Seasonal averages, calculated from 25 years of coupled spinup
Prognostic variables	Surface pressure, horizontal wind, total water mixing ratio, liquid water potential temperature
Climate sensitivity	2.5°C

The performance of HadCM2 in simulating present climate has been evaluated among others by Johns et al. (1997; global point of view) and Räisänen and Döscher (1999; focus in northern Europe). The model does have its weaknesses, but it is still probably one of the best present GCMs in simulating current climate. In addition, the large-scale temperature and precipitation response of HadCM2 to increased CO_2 is relatively close to the average response of several other global models, both in the global mean and in the Nordic region (SWECLIM 1998, Fig. 2). If the response of the real climate system to increased CO_2 is close to the average response of climate models is, of course, still unknown.

2.2 RCA – the Rossby Centre regional Atmospheric climate model

The first version of the Rossby Centre regional Atmospheric climate model (RCA) is described by Rummukainen et al. (1998). RCA builds on a parallel coding of the operational High Resolution Limited Area Model HIRLAM, version 2.5 (Källén 1996; see also Machenhauer 1988 and Gustafsson 1993). The first RCA domain was set with a rotated Arakawa C latitude/longitude grid having a resolution of 0.4° (44 km) with 82 points in latitude and 114 points in longitude. The lateral forcing from the driving HadCM2 model was applied using 8-point lateral relaxation zones. The 19 vertical levels, set in hybrid coordinates, were the same as in HadCM2.

The model advection is Eulerian with a 5 minute time step. A three time-level semi-implicit scheme is used (after Simmons and Burridge 1981). The explicit dynamical part (advection, horizontal diffusion) is computed with a leap-frog scheme for wind, temperature and specific humidity and with an upstream scheme for cloud water. Vertical advection treats temperature and specific humidity, but not cloud water. The explicit fourth-order horizontal diffusion operates on model levels on wind and along pressure levels on temperature and specific humidity.

Vertical diffusion of momentum, dry static energy and moisture is based on the similarity theory in the surface layer and on the K-model above the surface layer (Louis 1979; Louis et al. 1981; Geleyn 1987). The roughness lengths for land points are prescribed. Over sea, the Charnock formula is used with the Charnock constant set to 0.018. The wind speed dependencies of sensible and latent heat fluxes over sea are reduced by using the formulation of Makin and Perov (1997).

The convection scheme is of the Kuo (1965, 1974) type. The microphysical calculations are from Sundqvist et al. (1989) and Sundqvist (1993). The total concentration of cloud water and cloud ice is predicted, but the division between these is diagnostic. Convective condensation occurs when both the temperature is below the moist adiabatic value above the lifting condensation level (LCL) of surface air and there is water vapour convergence. If there is no convection, stratiform condensation can start in a cloud free grid box if relative humidity exceeds a threshold value, which varies with altitude and is different for sea and for land.

The radiation parameterization is from Savijärvi (1990), modified further by Sass et al. (1994). The scheme has only two spectral intervals, one for short-wave (solar) and the other for long-wave (terrestrial) radiation. The short-wave part includes crude contributions from O_2 , CO_2 , O_3 , H_2O and aerosol absorption and scattering. Cloud absorption and transmissivity formulations use the calculated cloud water. The surface albedo varies according to surface type (water, ice, open land or forest, snow). The long-wave part is based on an empirical water vapour emissivity function (Savijärvi

1990). The total radiative effect in the long-wave is a combination of the clear sky contribution and three different cloud configurations for clouds in the grid box, as well as below and above it. The model-calculated water vapour distribution and cloudiness are used. The contributions from other trace gases than water vapour (CO_2 , O_3) are taken as constants.

The soil scheme is a modified version of the old three-layer ECMWF scheme (see e.g. Blondin 1988). The scheme is of the force-restore type and it is closed from below with prescribed monthly deep-soil temperature and moisture values, which are derived from the driving global model. The soil water is constrained not to exceed a maximum value (field capacity). Excess is removed as point runoff. To take the geographical variations in thermal and hydraulic soil properties into account, the nine FAO-Unesco (1981) soil types (Bringfelt et al. 1995) have been introduced. The heat capacities, heat diffusivities, and hydraulic diffusivities depend on soil type and the calculated soil moisture. There is no representation of effects related to vegetation cover. A time evolution of the snow density is prescribed in RCA using values by Eerola (1996), which are for conditions in southern Fennoscandia.

The lateral boundary conditions, the temperature and moisture content of the deep soil, and sea surface temperatures (SSTs) for the first RCA climate simulations were taken from the driving HadCM2 model. In part of the model area, the ice cover was also taken directly from HadCM2. In northern Europe, however, ice cover was deduced from a proxy based on soil temperatures (Rummukainen et al. 1998). This formulation was adopted because the wintertime SSTs in the Baltic Sea in HadCM2 are too warm and keep the basin totally ice-free, and because the extrapolation of the HadCM2-simulated SSTs to inland areas also kept, in the first test runs, the numerous inland lakes in the Nordic region open even in the coldest winters (the extrapolation of SSTs was needed because HadCM2 has no lakes). The lack of ice in these test runs led to a substantial warm bias in winter temperatures.

2.3 The first two 10-year simulations

The first two 10-year RCA simulations derived their driving boundary data from two different integrations made with the HadCM2 model. In one of these (the control run), the atmospheric equivalent¹ CO_2 content in HadCM2 was kept at its preindustrial level. In the other (scenario run), increased equivalent CO_2 was prescribed. These two HadCM2 runs are reruns of earlier, much longer integrations made with HadCM2, namely the control run discussed by Johns et al. (1997) and the increased greenhouse gas run described by Mitchell and Johns (1997). The reruns were needed to provide the Rossby Centre and other regional climate modelling groups with the boundary data required for driving limited-area models – the data stored from the original simulations

¹ The radiation code in HadCM2 excludes trace gases like CH_4 , N_2O and the CFCs. In order to get the same global mean radiative forcing as CO_2 and these other well-mixed greenhouse gases would give together, the CO_2 concentration used in the model is higher than that in the real atmosphere.

were not detailed enough for this purpose. The reruns got their initial conditions from the original runs, but a different computer was used. Due to the nonlinear growth of the initial bit-level differences associated with this change, the climate in the reruns is not identical with the climate in the same period of the original runs. However, the differences seem to be within the normal internal variability of the HadCM2 model.

In the HadCM2 model time, the 10-year period used for the RCA simulations extends from September 2039 to November 2049. The equivalent CO₂ concentration in the scenario run during this decade is roughly 150% higher than the preindustrial value used in the control run². If one wishes to take the differences between the scenario run and the control run as indicators of the differences in real-world climate between the present and some future, this future is for two reasons more likely to be around 2100 than in 2039-2049. On one hand, the control run neglects the increase in greenhouse gases from the preindustrial time to the present, and, on the other hand, the assumed increase in equivalent CO₂ after 1990 is relatively fast, 1% per year. The 10-year mean difference in global mean surface air temperature between the HadCM2 scenario and control runs in 2039-2049 is 2.6°C. This is close to the best estimate of Houghton et al. (1996) for the greenhouse gas-induced global mean warming between 1990 to 2100, which is slightly below 2.5°C³. Note that model results suggest the climate change caused by a certain accumulated increase in CO₂ to be only weakly sensitive to the time history of the forcing, i.e., how fast CO₂ has been increased (Houghton et al. 1996, pp. 312-314).

The present version of RCA describes the radiative effects of CO₂ in a highly parameterized way, with a few numerical constants associated with the transport of solar and terrestrial radiation. As it was difficult to estimate how these constants would change with increasing CO₂ (and changing climate, including more atmospheric water vapour), the same HIRLAM-based constants were used in the scenario run as in the control run. It was reasoned that the direct radiative effect of increased CO₂ within the RCA domain would be of secondary importance, because RCA is strongly forced by the driving global model from both the lateral boundaries and from below (sea surface and deep soil temperatures). In addition, the major positive feedback associated with the effect of increased water vapour to long-wave radiation is included explicitly even in RCA. The results of the first climate change simulation suggest that this reasoning was largely correct, because RCA simulates climate changes similar in magnitude with those in HadCM2. Nevertheless, the lack of a CO₂ increase appears to have a clear signature in the behaviour of one parameter, outgoing long-wave radiation (section 3.6). It might

² In the original scenario run, the equivalent CO₂ concentration is based on observed greenhouse gas concentrations until 1990 and increases exponentially 1% per year after that.

³ This figure is obtained by combining a central scenario of future greenhouse gas emissions, IS92a, with the best estimate of the climate sensitivity parameter that gives the equilibrium change in global mean surface air temperature due to a doubling of CO₂ (2.5°C). Notably, the latter coincides with the sensitivity of HadCM2 (see Table 1).

therefore have a minor impact on other aspects of simulated climate change as well, although it is impossible to quantify this from comparison with HadCM2 alone.

One of the facts one must keep in mind in interpreting the model results is that increases in CO₂ and other well-mixed greenhouse are only one, although presumably the most important, of the forcing factors that may induce climate changes in the next century. Other examples, neglected in the present model simulations, include future changes in anthropogenic aerosols (difficult to estimate because tropospheric aerosols are short-lived) and natural forcing factors like solar variability and volcanic eruptions.

2.4 Climate in the RCA control simulation

The climate in the RCA 10-year control simulation was documented by Rummukainen et al. (1998), with the main emphasis on the conditions near the surface. Comparison was made on one hand with the driving HadCM2 simulation, on the other hand with the present (1961-1990) observed climate. Comparison of the control run with the present climate is slightly inconsistent in the sense that the equivalent CO₂ in the driving model was at its preindustrial level. Generally speaking, however, we expect the low equivalent CO₂ content to be only a secondary cause of the differences between the modelled and observed climate.

Below follows a summary of some of the main findings in Rummukainen et al. (1998). The list naturally includes several shortcomings of the model, but on the whole the results of this first extended control simulation appear quite encouraging.

2.4.1 Circulation and atmospheric temperatures

- RCA has a general cold bias in lower tropospheric (and in summer, midtropospheric) temperatures relative to the driving HadCM2 model, which itself is generally colder than the observed climate, particularly in summer. The difference is small in the area mean sense (at 850 hPa, 0.5°C in annual mean) but somewhat larger over central Europe especially in summer. The geographical distribution of this temperature difference is such that it directs (through the thermal wind relationship) the upper tropospheric west wind maximum to be slightly further to the south in RCA than in HadCM2.
- The intraseasonal variability of sea level pressure is slightly smaller in RCA than in HadCM2, in particular in northern Europe in summer.

2.4.2 Surface air temperature

- In comparison with observations, the seasonal mean surface air temperatures in RCA are of similar quality with those in HadCM2. HadCM2 suffers from a cold bias of 2-4°C in northern Europe in summer and this is only slightly reduced in RCA. In most other respects, RCA is the colder of the two models. In general, the differences between the two models and the observed climate are reasonably small.

at least when compared with the much larger biases in some earlier GCM simulations (Räisänen 1994).

- Diurnal temperature variability in RCA in northern Europe is slightly smaller than that observed. In some rare winter situations, however, the model simulates extremely cold temperatures, probably as a result of unrealistically sharp surface inversions.

2.4.3 Precipitation and surface hydrology

- Annual mean precipitation in northern Europe is reasonably well simulated. In both the annual and seasonal means, the higher horizontal resolution allows RCA to capture the geographical distribution of precipitation considerably better than HadCM2 does.
- The seasonal cycle of precipitation in Sweden in RCA is flatter than that observed in 1961-1990, with more precipitation in winter and spring and less in summer. The disagreement is, however, in part caused by biases in observations (the measurements are known to give a substantial underestimate of solid forms of precipitation) and it may also be affected by the shortness of the simulated period. The seasonal cycle of precipitation in Sweden in the driving HadCM2 model is in this decade equally flat as it is in RCA, but it is somewhat more pronounced in the original 240-year HadCM2 control run (Räisänen and Döscher 1999; see also Section 6 of this report).
- At least in Sweden, RCA overestimates the number of days with light precipitation, and to some extent underestimates the number of days with heavy precipitation.
- Despite a reasonable annual mean precipitation, both annual mean evaporation and runoff in Sweden are below the climatological estimates in Raab and Vedin (1995). Relaxation to deep soil moisture fields taken from HadCM2 allows the surface scheme to lose water, in Sweden of the order of 100 mm per year.

2.4.4 Total cloudiness

- RCA has a tendency to overestimate cloud cover in northern Europe in winter and spring. It also appears to develop an orographic maximum of cloudiness that is too strong over the Scandinavian mountains. Otherwise, the agreement with observations is reasonably good and mostly better than in the case of the HadCM2 control simulation.

2.4.5 Snow and ice cover

- The ice climate of the Baltic Sea is reasonably close to that observed, although this has been achieved with a somewhat unphysical parameterization. Similar conclusion applies to the ice cover in inland lakes.
- The simulated snow climate is at least in Sweden in good general agreement with observations, in terms of both the duration of the snow season and the water storage of the snow pack. However, the agreement may hide compensating errors in the

form of too fast snow melt countered by abundant winter precipitation and cool springs.

3 Comparison of climate changes in RCA and HadCM2

In this and the following section, several aspects of the simulated climate changes are discussed. Climate changes are here defined as 10-year (December 2039–November 2049) mean annual, seasonal or monthly differences between the climates in the scenario run and in the control run. The first three months of the RCA simulation are neglected to avoid initial spinup effects associated with the soil model.

The fact that the control run and the scenario run are both only 10 years long calls for certain additional care in interpreting the model results. In climatic averages of such limited length, considerable variations may occur as a result of internal variability even with constant external forcing conditions. Therefore, we will systematically check the statistical significance of the simulated climate changes. For this, we use the standard t statistics, defined here as

$$t = \frac{X2 - X1}{\sqrt{(V1 + V2)/9}}$$

where $X1$ and $X2$ are the 10-year means of variable X in the control run and in the scenario run, and $V1$ and $V2$ the interannual variances of X within these two runs. This definition assumes that X is normally distributed and its values in subsequent years are uncorrelated. For most of the parameters studied here, neither of these assumptions should be severely violated. In some cases, however, the assumption of zero interannual autocorrelation might make the significance estimates slightly nonconservative, so that the null hypothesis of no change between the two model runs is rejected too easily. A typical example of a parameter that might have non-negligible interannual memory is surface air temperature over the Atlantic Ocean.

In the maps shown in this report, two threshold values for the absolute value of t are used: 1.734 for two-sided significance at the 90% level, and 2.878 for two-sided significance at the 99% level. By definition, one would expect to find an average amount of 10% (1%) of differences significant at the 90% (99%) level even when comparing two model runs with identical forcing (provided that the runs differ, for example, in their initial state). In practice, one can claim the signal to be well discernible from the noise only when the proportion of significant changes is considerably larger than its expected value in the absence of external forcing.

Self-evidently, the t test only measures the significance of the simulated climate changes against the internal variability in the used HadCM2–RCA model configuration. Some of the changes that have according to this test high statistical significance might,

therefore, be completely different if a different global model and/or a different regional model were used.

3.1 Atmospheric circulation

Figure 1 shows the 10-year seasonal mean changes from the RCA control to the scenario run in four variables characterizing the atmospheric circulation near the surface and in the free atmosphere: sea level pressure, 500 hPa height, 850 hPa temperature and the zonal wind component at 300 hPa. The four three-month seasons are denoted as DJF (December-February), MAM (March-May), JJA (June-August) and SON (September-November).

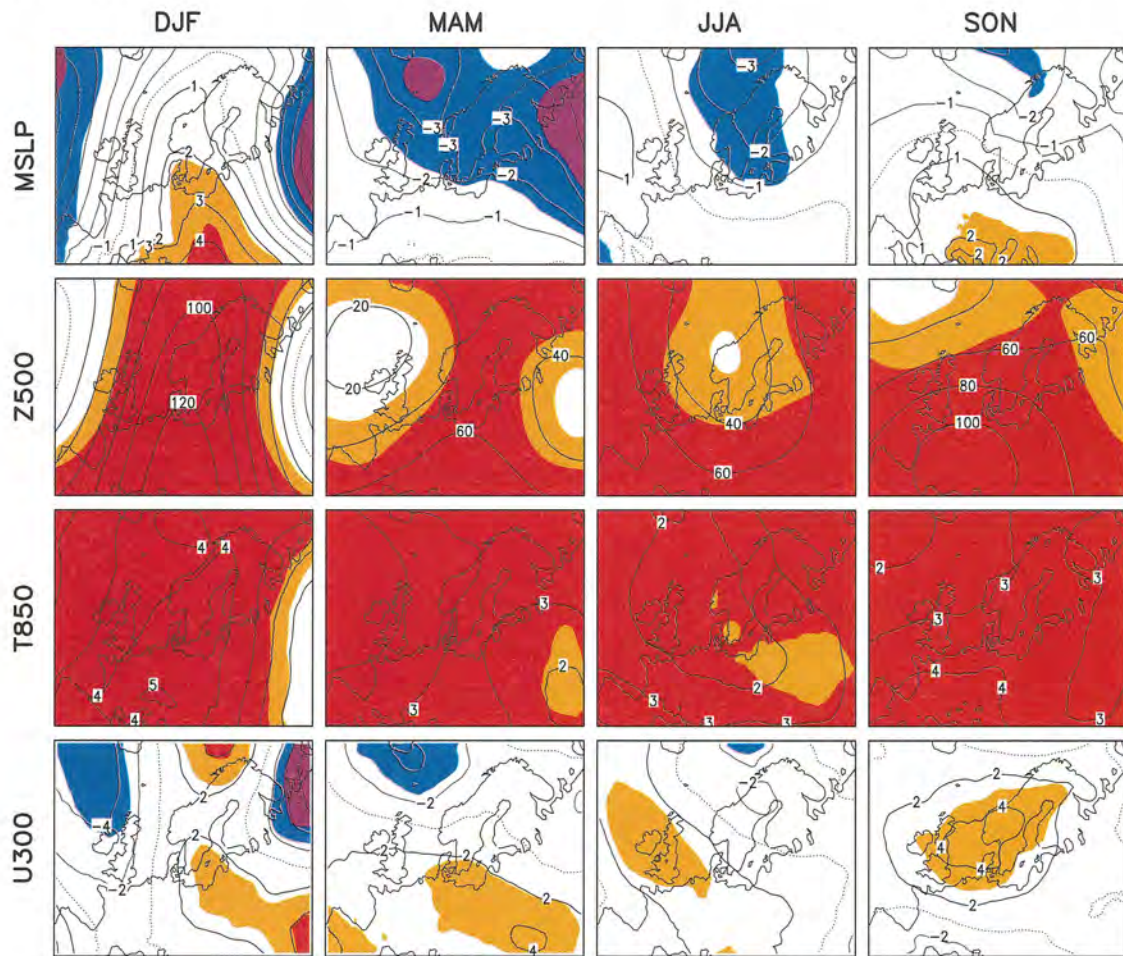


Figure 1. 10-year seasonal mean changes (RCA scenario - RCA control) in mean sea level pressure (MSLP; contours every 1 hPa), 500 hPa height (Z500; every 20 m), 850 hPa temperature (T850; every 1°C) and 300 hPa zonal wind (U300; every 2 m s⁻¹). Zero lines are stippled. Positive changes significant at the 90% (99%) level are shaded in orange (red), and negative changes significant at the 90% (99%) level in blue (violet). The maps show the whole RCA model domain excluding the 8-point boundary relaxation zones.

An evident change from the control run to the scenario run is that the troposphere is warmer in the latter. At 850 hPa, the difference in the RCA domain is 2-3°C in summer

and spring, 2-4°C in autumn, and from less than 1°C near the eastern boundary to 5°C in central Europe in winter. With the exception of the eastern boundary in winter, the changes are statistically significant at least at the 90% level, generally even at the 99% level. The warming is directly reflected in a general increase in 500 hPa heights, which is likewise statistically significant in most of the model domain in all seasons.

The changes in time mean sea level pressure are more subtle. A general feature is a somewhat increased north-south gradient over southern Scandinavia and northern parts of central Europe, which indicates a strengthening of westerly flow near the surface in these areas. However, the details vary greatly from season to season. In spring and summer, the pattern of change indicates a more cyclonic surface circulation over the Nordic area, whereas the pattern in winter is dominated by a ridge extending northward from central Europe. The increased northerly flow between this ridge and an area of pressure decrease further east is very likely an explanation for the modest warming in the eastern part of the model domain. In general, however, the changes in sea level pressure are less discernible from internal variability than those in 850 hPa temperature and 500 hPa height.

The difficulty of separating the signal from the noise is similar with respect to the changes in 300 hPa zonal wind. Nevertheless, just as was inferred for the lower troposphere from the changes in sea level pressure, the upper tropospheric westerly winds over southern Scandinavia and Central Europe become slightly stronger. This change is largest in autumn.

The changes in these four variables in RCA are generally very similar to those in HadCM2. Some differences nevertheless occur, as illustrated for temperature changes in Fig. 2. In all seasons excluding winter, the warming at 850 hPa is generally slightly weaker in RCA than in HadCM2. In the eastern part of the model domain, the difference locally reaches 1°C in summer. Area means taken over all land grid boxes in the RCA domain (excluding the boundary relaxation zones) show largest intermodel difference in summertime warming in the lower troposphere – the difference at 2 m is even larger than that at 850 hPa. In spring, however, the maximum difference occurs at 500 hPa.

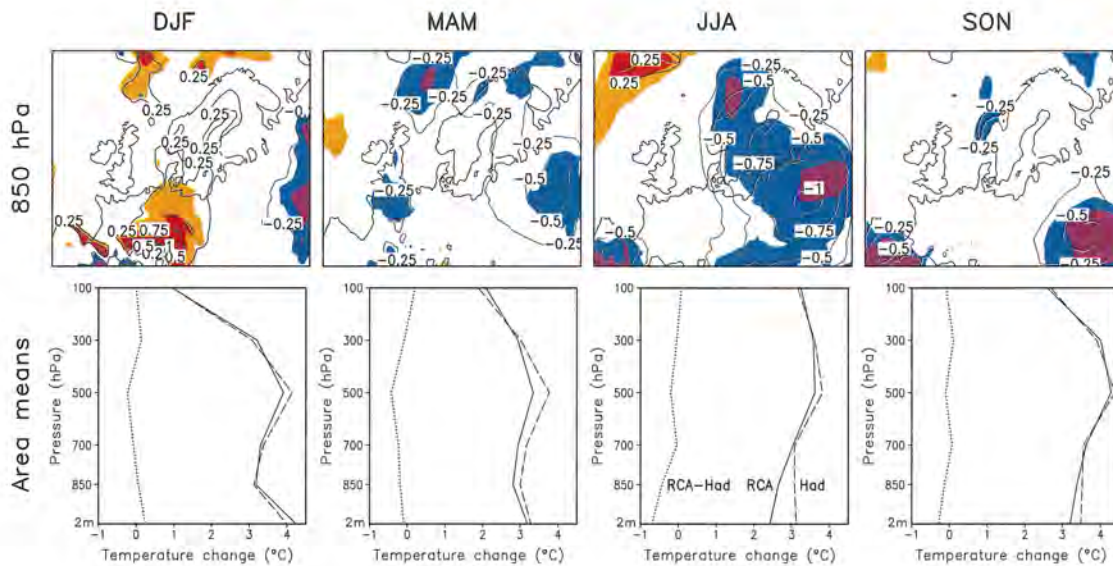


Figure 2. Top: 10-year seasonal mean differences RCA-HadCM2 in the change in 850 hPa temperature from the control run to the scenario run. Contours at $\pm 0.25^\circ\text{C}$, $\pm 0.5^\circ\text{C}$, $\pm 0.75^\circ\text{C}$ and $\pm 1^\circ\text{C}$. The shading indicates the statistical significance for the difference RCA-HadCM2 (colour scale as in Fig. 1). Bottom: Area mean temperature changes at five isobaric levels (100, 300, 500, 700 and 850 hPa) and at 2 m in RCA and HadCM2, and the difference RCA-HadCM2. The area means are taken over all land grid boxes excluding the boundary relaxation zones.

3.2 Surface air temperature

The simulated changes in surface air temperature in winter, summer and annual mean in both RCA and HadCM2 are shown in Fig. 3. The statistical significance of these changes is generally high and is not shown explicitly.

The general distribution of the simulated annual mean warming in the two models is very similar. In both RCA and HadCM2, the warming is weak (locally below 1°C) over the northern North Atlantic, where the similarity of the results is dictated by the use of the HadCM2-simulated SSTs even in RCA. Over much of Europe, the warming is $3\text{--}4^\circ\text{C}$, and in parts of northern Europe it exceeds 4°C in both models. The annual area means taken over all land grid boxes in the RCA domain are 3.3°C in RCA and 3.5°C in HadCM2.

In the finer details, there are some obvious (and in fact statistically significant) differences between the models. Perhaps the most striking of these is the strong local maximum of warming in RCA over the northern parts of the Baltic Sea, which is totally absent in HadCM2. This maximum is visible even in the annual mean, but it is most pronounced in winter, when the warming in RCA locally exceeds 10°C over the Bothnian Bay. This very strong warming results from a substantial decrease of sea ice in RCA (see Section 4.2), and it is felt to some extent even in the coastal areas of Finland and Sweden. However, as already mentioned, the existence of ice in RCA is inferred from a proxy based on soil temperatures. The ice cover in RCA is thus independent of the Baltic Sea SSTs, which are taken directly from HadCM2 and are warm enough to

keep the Baltic Sea in that model totally ice-free even in the control simulation. As discussed below, this calls for some care in the interpretation of the model results.

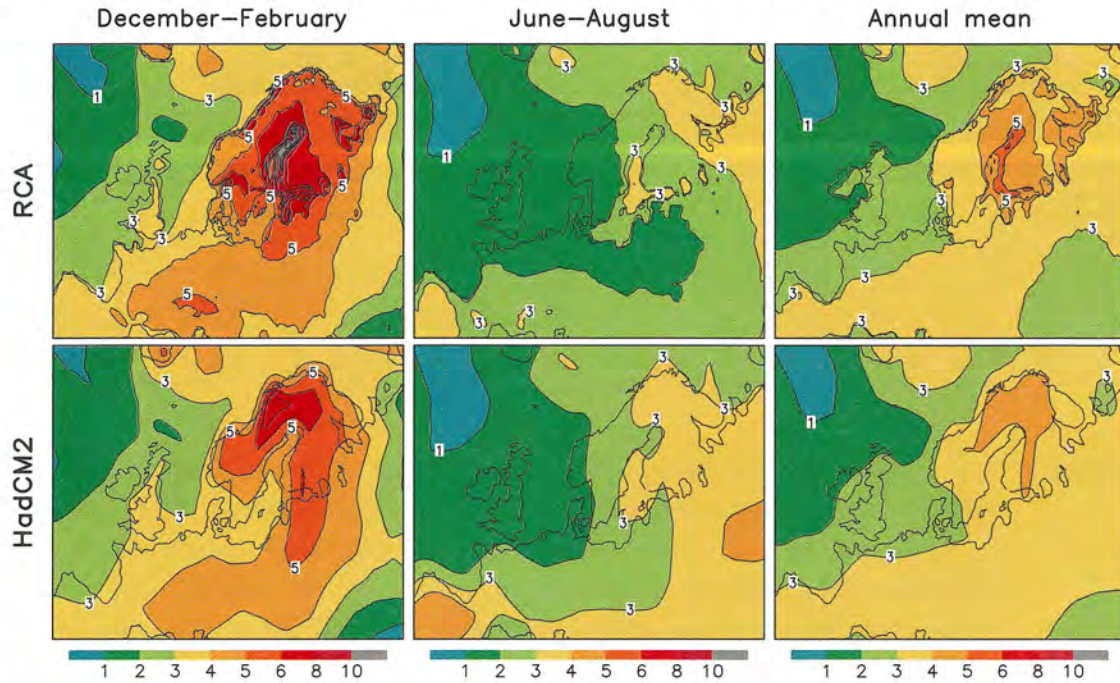


Figure 3. Simulated changes in surface air temperature ($^{\circ}\text{C}$) in RCA (top) and HadCM2 (bottom) in December-February, June-August and annual mean.

Figure 4 provides a closer look at the situation in one grid box in the Bothnian Bay (at approximately 23°E , 65°N). In the RCA control run, this grid box is ice-covered over 75% of time in January and February. The warm SSTs ($3\text{--}4^{\circ}\text{C}$) obtained from HadCM2 have therefore only a small effect on the surface air (2 m) temperatures above the ice, which sink below -11°C in January mean. In HadCM2, which has no ice cover, the January mean surface air temperature is -4°C . This is also several degrees colder than the SST, indicating that cold advection from surrounding land areas acts to maintain a very unstable near-surface temperature stratification. Nevertheless, the difference from RCA is substantial.

In the scenario run, ice never develops in this grid box even in RCA. Consequently, the time mean surface air temperatures in the two models are very similar (although in midwinter still several degrees colder than the SST, which in this run has a January mean of over 6°C). But, because air temperatures in the control run were much colder in RCA than in HadCM2, the change from the control run to the scenario run is much larger in RCA than in HadCM2.

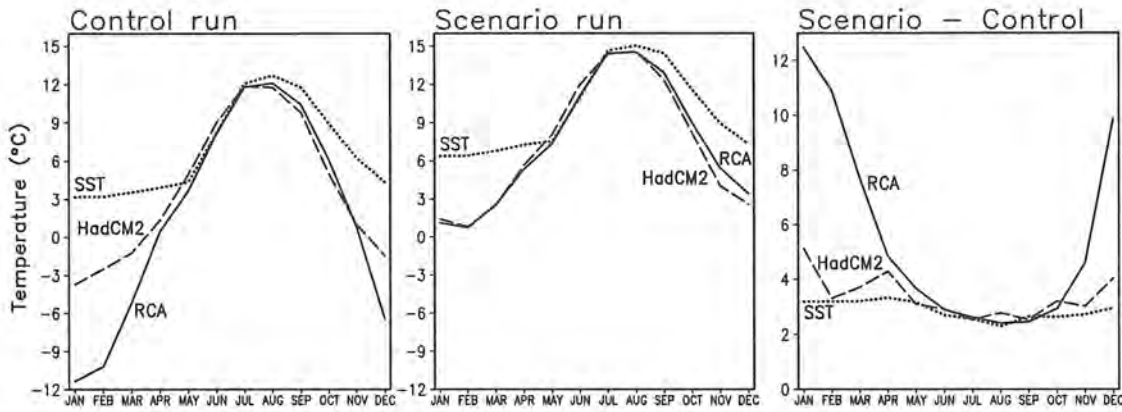


Figure 4. 10-year monthly mean SSTs in HadCM2 (dotted), and surface air temperatures in RCA (solid) and HadCM2 (dashed) in a grid box in the Bothnian Bay. The left panel shows the temperatures in the control run and the midpanel those in the scenario run, and the right panel the difference between the scenario and control runs.

As far as the decrease in ice cover is reasonable, the associated local enhancement of warming appears a qualitatively plausible feature. However, the magnitude of this effect in RCA may be too large. As a thought experiment, suppose that the SSTs in both the control and the scenario run had been 4°C colder (a change of about this magnitude in SSTs is needed to make them consistent with the soil-proxy-derived ice cover in RCA). With the same abundant ice cover, this would have had little direct effect on air temperatures in the control run. In the ice-free scenario run, however, 4°C colder SSTs would certainly have made the air temperature lower, although presumably by less than 4°C (because the air temperature is affected both by the SST and advection from surrounding land areas, and the latter is not changed directly). Therefore, if the SSTs had been consistent with the ice cover, the air temperature increase in RCA would have been somewhat smaller, although it is difficult to estimate how much. Clearly, this stresses the importance of having a physically self-consistent treatment of the Baltic Sea and its ice cover in the next RCA simulations.

While the warming in winter in RCA is similar, or around the Baltic Sea larger than that in HadCM2, the warming in summer and early autumn is generally smaller in RCA than in HadCM2. Thus, the contrast between strong warming in winter and weaker warming in summer is more pronounced in RCA than in HadCM2 (see also the area means in Fig. 12). In parts of eastern Europe and Spain, the intermodel difference in summertime warming exceeds 1.5°C. In these areas, the RCA simulation is the cooler of the two even in the control run, and in the scenario run the difference grows larger – not since the warming in RCA would be particularly weak but rather since the warming in HadCM2 is strong. A look at the changes in surface energy balance in the two models reveals that, in both of these areas although more markedly in Spain, decreased cloudiness in HadCM2 leads to an increase in the solar radiation available at the surface. In RCA, the increase in solar radiation in Spain is smaller and the change in eastern Europe is close to zero. In addition, drying of soil in HadCM2 leads in Spain to

a substantial increase in the surface sensible heat flux at the expense of latent heat flux, while in RCA both latent and sensible heat fluxes increase. A similar though smaller difference between the models occurs in eastern Europe.

Another factor that may act to make the warming in RCA weaker than that in HadCM2 is the neglect of CO₂ increase in the RCA radiation scheme. The effect of this seems to be clearly visible in the top-of-atmosphere radiation budget (Section 3.6). However, it is more difficult to estimate its contribution to the generally slightly weaker warming in the free troposphere in RCA than in HadCM2 and to the seasonally varying intermodel differences in surface air warming.

3.3 Precipitation

The relative changes in precipitation in the two models in winter, summer and annual mean are shown in Fig. 5. As they should, the large-scale patterns of change in RCA and HadCM2 are quite similar. Annual mean precipitation increases in northern Europe in both models, and this increase has at most locations a relatively high statistical significance. Decreases of annual mean precipitation occur locally in both models in the southern part of the RCA model domain and over the northern North Atlantic, and in RCA near the eastern boundary.

Increases of precipitation dominate over decreases in both models in both winter and summer. Averaging over all land areas, the increase is somewhat larger in the first than in the second half-year (see Fig. 12), but in northern Europe there is little evidence of any systematic seasonal cycle. One of the very largest seasonal mean changes is a substantial increase in summer precipitation over the Baltic Sea – locally up to a doubling in both RCA and HadCM2. In considering this kind of seasonal details, however, it is essential to recall the limited length of these experiments. Although the simulated seasonal changes are frequently larger than the annual mean changes, their statistical significance is typically worse, because the natural variability of seasonal means is much larger than that of annual means. Analysis of longer HadCM2 simulations (Section 6) indicates that some of these details would most likely have been different if a longer downscaling experiment had been made. In summer, for example, increase in precipitation in northern Europe as whole would probably have been smaller, and the strong local maximum over the Baltic Sea would have been less pronounced.

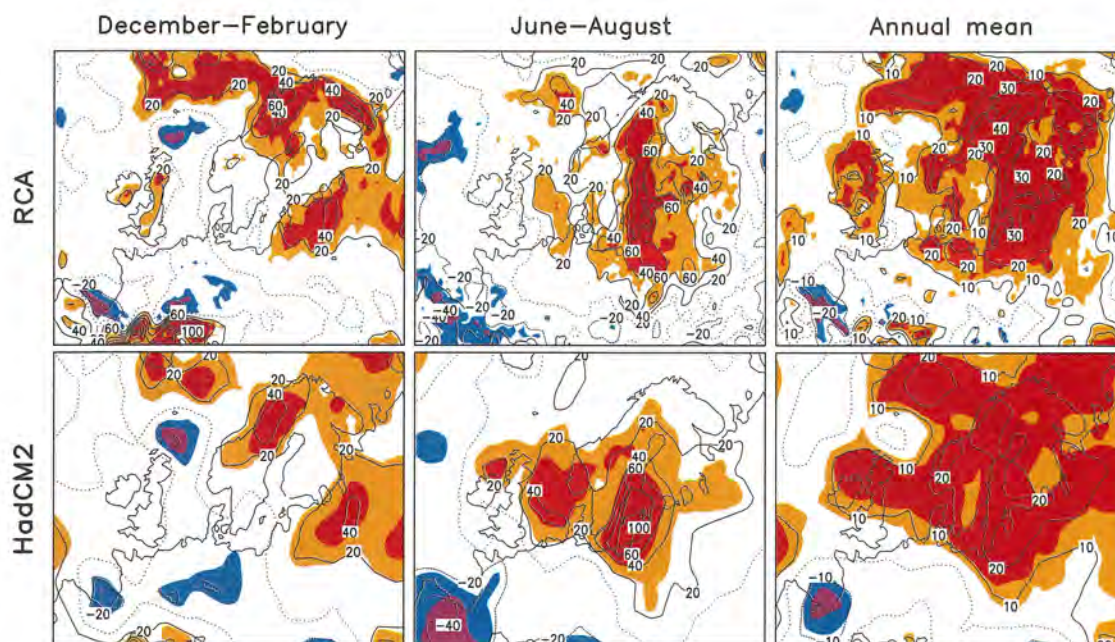


Figure 5. Simulated changes in precipitation in RCA (top) and HadCM2 (bottom) in December-February, June-August and annual mean. The contours express the change as per cent of the precipitation in the control run (interval 20% for seasonal and 10% for annual means; the zero contour is stippled). A slight horizontal smoothing has been applied to the RCA results to enhance readability. Increases significant at the 90% (99%) level are shaded in orange (red), and decreases significant at the 90% (99%) level in blue (violet).

In the finer geographical details, differences between the precipitation changes in RCA and HadCM2 exist. For example, the increase in annual mean precipitation in northern Sweden is 30-40% in RCA, but only around 20% in HadCM2. In addition, the area of increasing precipitation extends in summer and in annual mean somewhat further south in central Europe in RCA than in HadCM2. Likewise, RCA simulates much sharper gradients in the change in winter precipitation around the Alps than HadCM2. It turns out, however, that the differences in the precipitation response of the two models are only rarely statistically significant, at least at the local and seasonal level (Section 5).

3.4 Total cloudiness

As compared with the relatively close similarity between RCA and HadCM2 in the changes in temperature and precipitation, the intermodel differences in the changes in cloudiness are surprisingly large, in particular in winter (Fig. 6). RCA simulates a substantial (locally 6-9% of sky) decrease in winter cloudiness in a wide area extending from Finland and Sweden over the Baltic Sea to central Europe. In HadCM2, by contrast, the changes in the same area range from small decreases to increases of up to 6%. In summer, the two models are in better agreement exhibiting decreased cloudiness in the southwestern and eastern parts of the RCA domain and slightly increased cloudiness around the Baltic States and southern and central Scandinavia. In this season,

however, the changes are less commonly statistically significant than in winter. In the annual mean, the land area mean change is -2.1% in RCA but negligible (-0.2%) in HadCM2. With the exception of reduced cloudiness over the Baltic Sea in RCA, annual mean changes over sea are relatively small in both models.

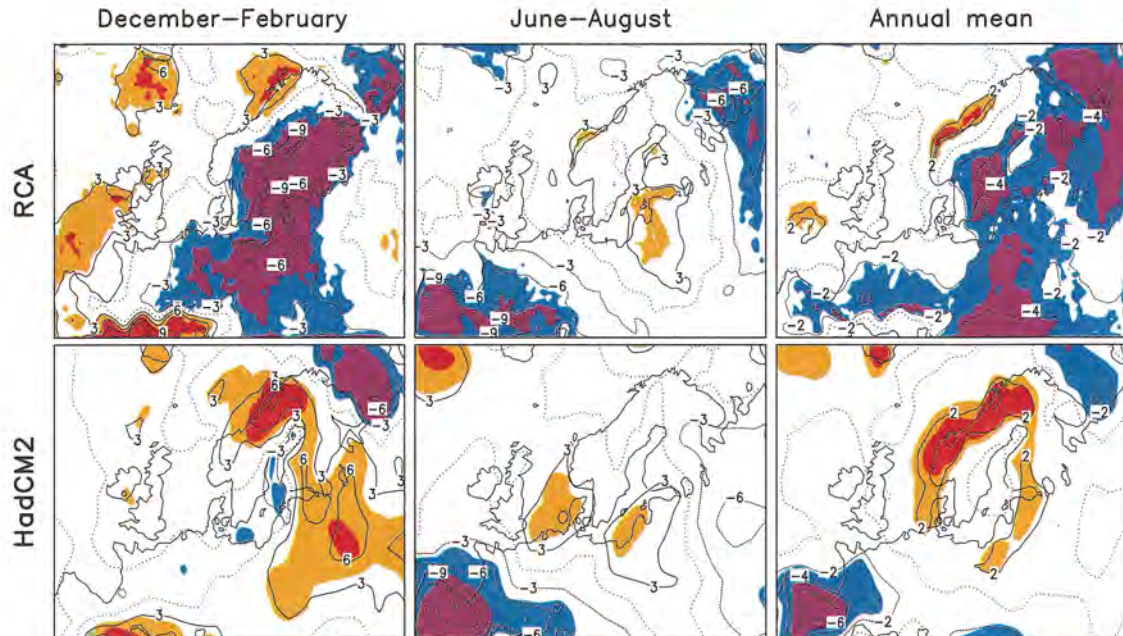


Figure 6. As Fig. 5, but for changes in total cloudiness (per cent of sky). Contours are drawn at every 3% in the maps for DJF and JJA, and at every 2% in the maps for annual mean changes.

The largest decrease of winter cloudiness in RCA occurs over the Baltic Sea, in particular over the northern parts of it, and coincides with a substantial decrease in ice cover. A possible explanation of this is that the model is more willing to create low-level stratus clouds in the typically stable conditions over ice than in the much more unstable conditions over open water. In the control run, at least, clouds at the lowest model level (essentially fog) are most common over those parts of the Baltic Sea that are most frequently covered by ice (cloud cover at other model levels was not saved, so it is not known if this conclusion holds higher up). In surrounding land areas, decrease of snow might play a similar role. Whether the response of RCA is physically correct is, however, not clear. For example, one might argue that decreased ice should rather increase than decrease low cloudiness (e.g., evaporation from open water is much larger than evaporation from ice).

Due to the obscurity of the physical mechanisms, the large differences between RCA and HadCM2 in changes in wintertime total cloudiness are more appropriately regarded as a sign of uncertainty than as a demonstration of how higher resolution allows a more realistic regional response.

3.5 Mean wind speed at 10 m height

The first two rows in Figure 7 show the simulated changes in mean wind speed at 10 m level in RCA and HadCM2. The changes in summer are relatively small in both models and of generally weak statistical significance. In winter and annual mean, however, RCA simulates a widespread increase in windiness in the Nordic region and in the eastern part of central Europe. A general increase in windiness in these areas takes place in HadCM2 as well, but this has a smaller magnitude. The difference is largest over the northern parts of the Baltic Sea (where the increase in DJF mean wind speed locally reaches 60% or 3 m s^{-1} in RCA!), but it is substantial in Sweden and southern Finland as well.

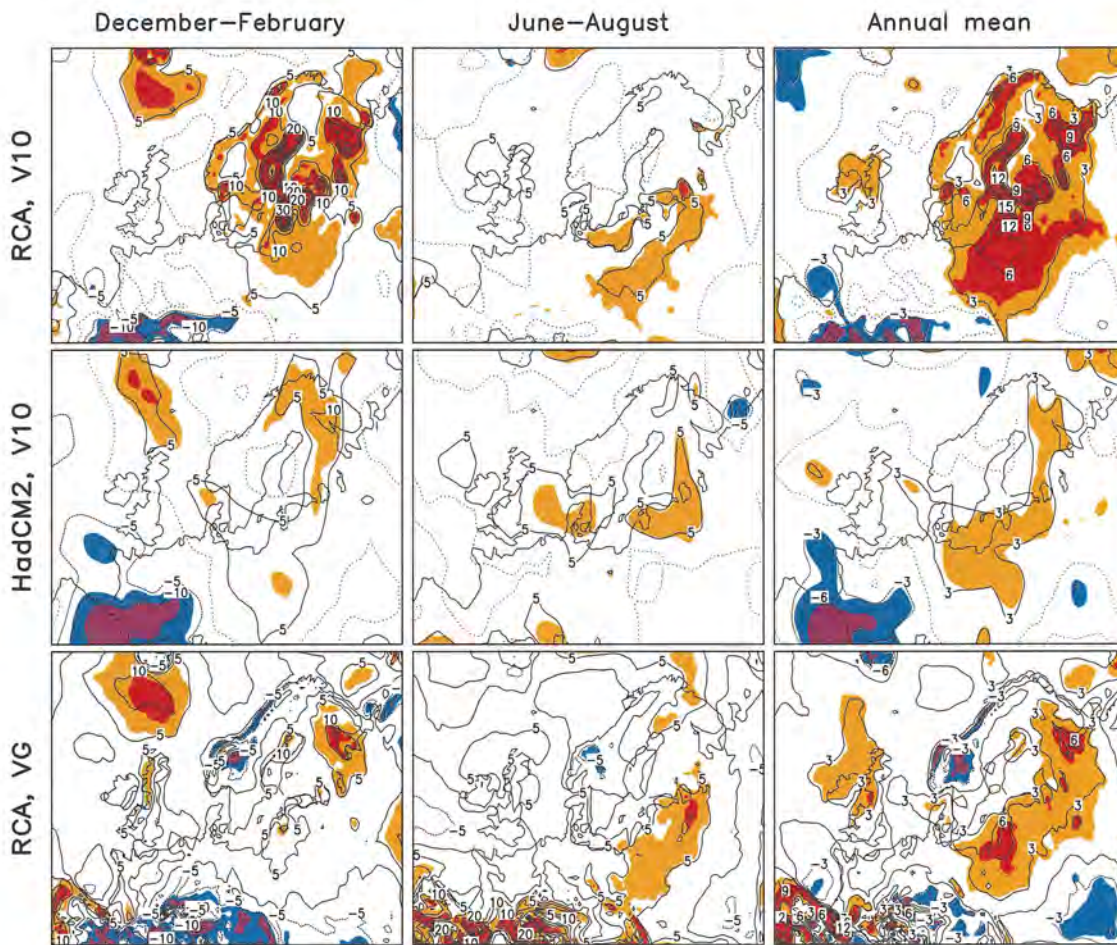


Figure 7. Changes in mean wind speed at 10 m height (in per cent of the mean wind in the control run) in RCA (top) and HadCM2 (middle), and the change in the mean surface geostrophic wind speed in RCA (bottom, see text). Contours at every 5% in the maps for DJF and JJA, and at every 3% in the maps for annual mean changes. Increases significant at the 90% (99%) level are shaded in orange (red), and decreases significant at the 90% (99%) level in blue (violet).

However, the origin of the large increase in wintertime windiness in RCA in northern Europe deserves some discussion. While one might expect such a change to be caused

primarily by sharpened pressure gradients, this does not seem to be the case. In the RCA experiment in the Nordic region in winter, changes in the time mean near-surface geostrophic wind speed (estimated from six-hourly time series of sea level pressure⁴) are significantly smaller than the changes in the actual 10 m wind speed (compare the bottom and top rows of Fig. 7). Thus, as shown in Fig. 8, the ratio between the actual 10 m wind speed and the geostrophic wind speed in the RCA simulation increases considerably in northern Europe in winter, with largest change in the northern parts of the Baltic Sea. In summer, the changes in geostrophic wind speed and the actual 10 m wind speed in RCA are much closer each other, as also indicated by the modest changes in the ratio between actual and geostrophic wind speeds in Fig. 8.

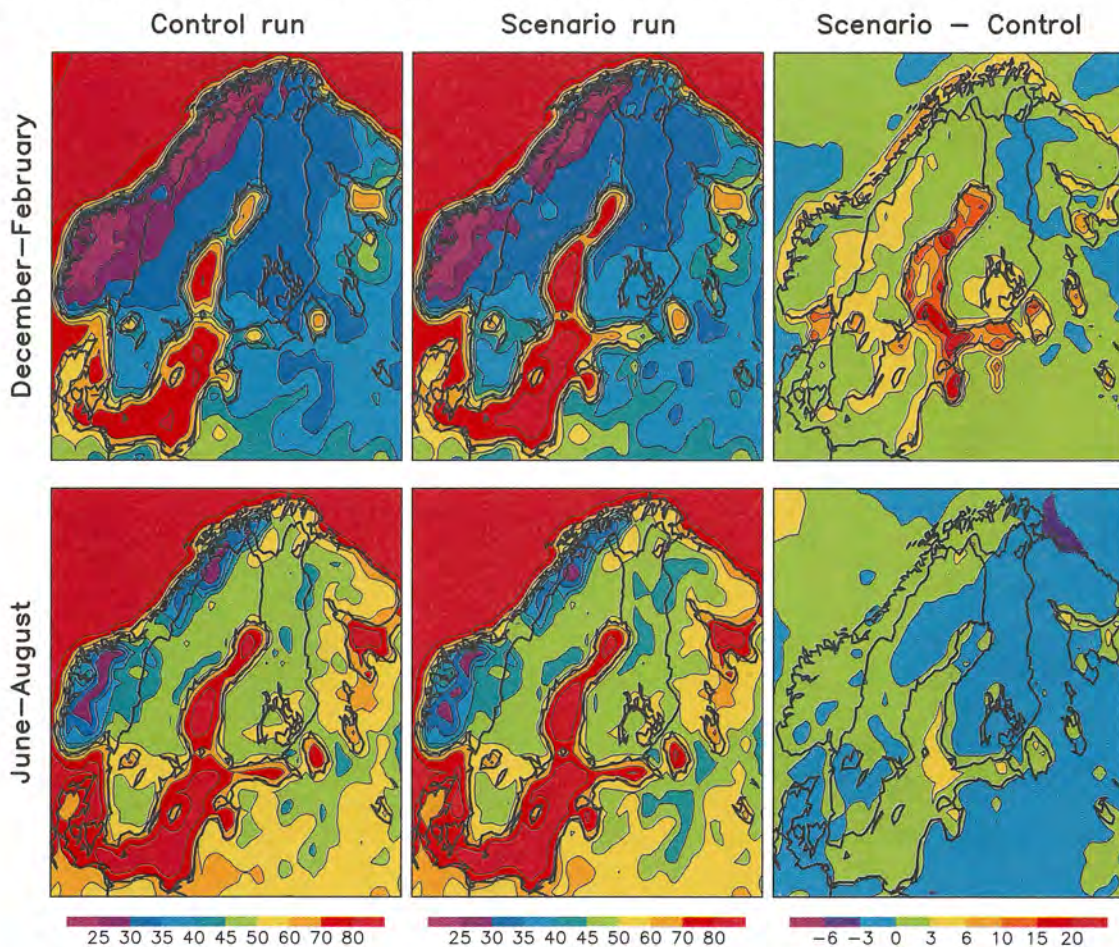


Figure 8. Ratio (multiplied by 100) between the mean 10 m wind speed and the mean geostrophic wind speed in northern Europe in December-February and June-August in the RCA control run (left) and scenario run (middle), and the difference between the scenario run and the control run (right).

⁴ This method gives good results only over low topography. The calculated geostrophic winds over mountainous areas appear to be too strong, because extrapolation of pressure from high altitude to sea level gives questionably sharp horizontal gradients.

The most plausible explanation for the large wintertime increase in windiness over the Baltic Sea is the effect of ice cover on surface layer stability. In the typically stable conditions over the frequently ice-covered Baltic Sea in the control run in winter, the ratio between the actual 10 m wind speed and geostrophic wind speed is much lower than it is in the control run in summer or in the largely ice-free scenario run in winter. Over the Gulf of Finland, for example, this ratio is in the control run in winter just slightly larger than over the surrounding land areas. It thus appears that, in sufficiently stable conditions, RCA simulates quite weak 10 m winds even over very smooth terrain. The weakening of near-surface winds with increasing stability is qualitatively reasonable, but it is not clear if this effect is as strong over ice cover in nature as it is in RCA. It might also be that the thermal stratification in RCA over sea ice is actually too stable, for example because, when ice exists, it always covers the whole grid box (thus, there are no leads).

The general, though much smaller, wintertime increase in 10 m wind speeds in land areas of northern Europe is also difficult to explain by any other means than a stability-related effect. However, the mechanisms over land appear to be of more delicate nature than over the Baltic Sea. Simple measures like the DJF mean temperature difference between the surface and the lowest model level show little evidence of decreased time-mean surface layer stability over land, in contrast with a dramatic decrease over the Baltic Sea. On the other hand, the boundary layer as a whole appears to become less stable even over land (compare the temperature changes at 2 m in Fig. 3 and at 850 hPa in Fig. 1), which should make momentum exchange between the surface layer and the free atmosphere more efficient. Clearly, however, the connections between wind changes, stability changes and decreased snow and ice would require further investigation.

3.6 Radiation balance

In this section we study the changes (scenario run – control run) in the annual mean radiation balance at the top of the atmosphere (TOA) and at the surface in RCA and HadCM2. A similar analysis of other components in the surface energy balance is provided in the next subsection. The areally averaged seasonal cycles of these changes are shown in subsection 3.8 in Fig. 13. Finally, Table 2 in the same subsection gives the areally averaged annual means of both the changes and the values in the control run for these and several other parameters.

Changes in TOA net short-wave radiation are determined by changes in planetary albedo and mostly reflect changes in cloudiness and snow and ice cover. The patterns of change in both models resemble the changes in summertime cloudiness (compare Fig. 9 with Fig. 6; changes in cloudiness in winter play a smaller role because there is little incoming solar radiation in this season), with generally increased (decreased) net short-wave radiation where cloudiness decreases (increases). In RCA, a marked decrease in winter- and springtime surface albedo associated with a decrease in the Baltic Sea ice

cover leads to a local increase in net short-wave radiation that is absent in the HadCM2 simulation.

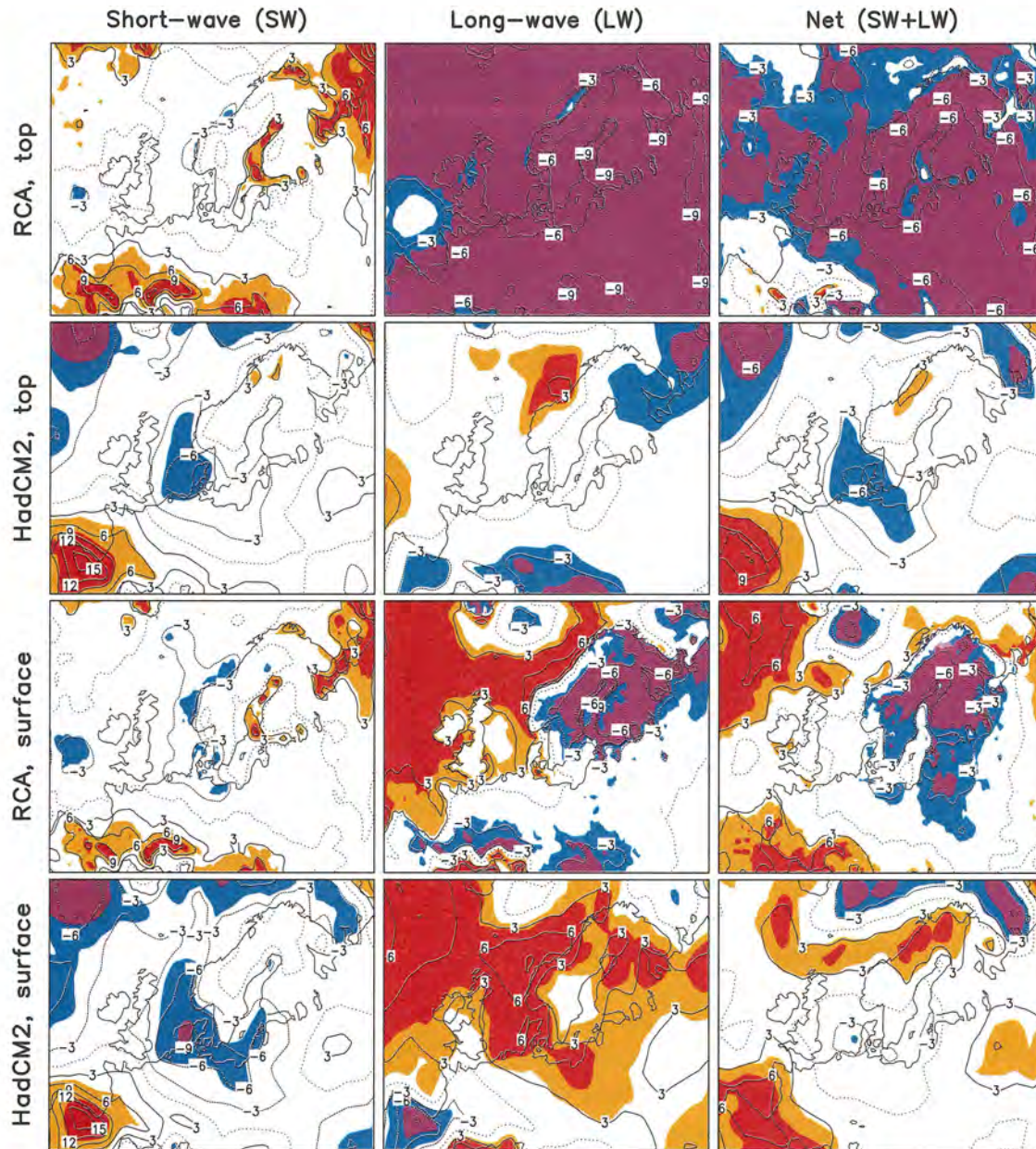


Figure 9. 10-year annual mean changes (scenario run – control run) in radiation balance (Wm^{-2}) in RCA and HadCM2 at the top of the atmosphere (first and second row) and at the surface (third and fourth row). Results are shown for changes in short-wave (left) and long-wave radiation (middle) and for the sum of these (right). All fluxes are defined positive downward (thus, for example, a negative change in top-of-atmosphere long-wave radiation balance indicates that outgoing long-wave radiation increases). Positive changes significant at the 90% (99%) level are shaded in orange (red), and negative changes significant at the 90% (99%) level in blue (violet).

Changes in TOA long-wave radiation differ more strongly between the models. In HadCM2, the changes are small and of varying sign. This indicates that the increase in tropospheric temperatures, which acting alone would make the outgoing long-wave radiation larger, is broadly compensated for by increased CO₂ and water vapour, which make it more difficult for the long-wave radiation to escape to space. Changes in cloudiness also affect this balance but (judging, for example, from the fact that there is very little change in the annual and area mean cloudiness in HadCM2) are probably of lesser importance. In RCA, however, the annual mean outgoing long-wave radiation increases in the whole model domain (with the sign convention in Fig. 9, a negative change indicates an increase in an upward directed radiation flux). As in HadCM2, the troposphere becomes warmer also in RCA and this is accompanied by a substantial increase in atmospheric water vapour – the change in the vertically integrated annual mean value averaged over the RCA domain is 24% in both models. Unlike in HadCM2, however, the increase in CO₂ is neglected in the RCA radiation code.

As averaged over the whole model domain, the annual mean net solar radiation at TOA in RCA increases by 1.7 Wm⁻², but the outgoing long-wave radiation increases by as much as 6.3 Wm⁻², giving a change of -4.6 Wm⁻² in the total TOA radiation balance. The same figures for HadCM2 are -0.4 Wm⁻², +0.5 Wm⁻² and -0.9 Wm⁻². The more negative change in the TOA radiation balance in RCA presumably contributes to the slightly weaker annual and area mean warming in the atmosphere and at the surface in RCA than in HadCM2. It is difficult to estimate the magnitude of this effect, but it would certainly be larger if the RCA model domain were larger and/or if the model were not forced from below by HadCM2-simulated SSTs and deep-soil temperatures.

The increase in outgoing long-wave radiation in RCA may of course be affected by factors other than the neglect of increased CO₂ in the radiation code. Some part of it is in fact likely to be associated with the slight tendency to reduced cloudiness in RCA. One may note, however, that the 6.3 Wm⁻² increase in outgoing long-wave radiation in RCA is only slightly larger than the global mean radiative forcing directly caused by increased CO₂ in the HadCM2 experiment. This is, judging from Table 1 of Mitchell and Johns (1997), close to 4.7 Wm⁻².

The changes in net (i.e., absorbed) short-wave radiation at the surface mirror in pattern the changes in net short-wave radiation at TOA. In both models, however, the changes at the surface are on the average 1-2 Wm⁻² more negative than those at TOA. This reflects a slight increase in atmospheric absorption presumably associated with increased water vapour.

In the HadCM2 experiment, the annual mean change in net long-wave radiation at surface is positive in most of the RCA domain (thus, the surface loses less heat by long-wave radiation). In RCA, the change is also generally positive over the northern North

Atlantic, where the surface warms relatively little. In most of the land area, however, the change in RCA is to the opposite direction. Even at the surface the change in net long-wave radiation is almost everywhere more negative in RCA than in HadCM2, although the area mean difference is smaller than at TOA (see Table 2). Presumably, both the different changes in cloudiness and the neglect of increased CO₂ in RCA contribute to the difference from HadCM2.

3.7 Surface energy balance

Annual mean changes in the surface total radiation balance (R) are redrawn in Fig. 10, together with the changes in sensible heat flux (H), latent heat flux (LE) and heat accumulation into the surface (R-H-LE). In HadCM2, a zero-heat-flux condition at the base of the soil model dictates the last term to be very small over land areas⁵. Over the Atlantic Ocean, however, the accumulation term is important in both models. Apart from some limited areas with relatively large SST increase such as that to the east of Iceland, the change in heat accumulation is generally positive over the northern North Atlantic. The warm sea water in this area releases large amounts of latent and sensible heat into the atmosphere in the control run. In the scenario run both the latent and sensible heat fluxes decrease, because the large heat capacity of the sea prevents the SSTs from warming as much as the atmosphere above.

In RCA, the accumulation term gets permanently nonzero although generally small values even over land areas. The heat flux at the soil base is not constrained to be zero but is rather determined by deep soil temperatures obtained from HadCM2. In addition, the land grid boxes in RCA (defined here as those in which the fraction of land exceeds 50%) have lakes within them, the surface temperature for the ice-free lake fraction being determined by the extrapolated HadCM2 SSTs rather than by energy balance requirements. The change in the accumulation term from the control run to the scenario run is in most of Europe marginally negative, in average over all land grid boxes by almost 1 Wm⁻². However, most of this extra heat appears to arrive in the atmosphere from lakes rather than from the soil, since the mean value for those grid boxes that have little (less than 5%) or no lakes is only -0.3 Wm⁻². The largest negative values occur in the lake-rich regions of northern Europe and are most likely associated with the shortening of the lake ice season. Similarly, the loss of ice causes the Baltic Sea release more heat to the atmosphere in the scenario run.

⁵ This could not be actually verified because latent heat flux over land in HadCM2 was not available. Instead, the latent heat fluxes shown in this report were derived assuming no heat accumulation into soil. This assumption is good for 10-year annual means but more approximate in the seasonal time scale.

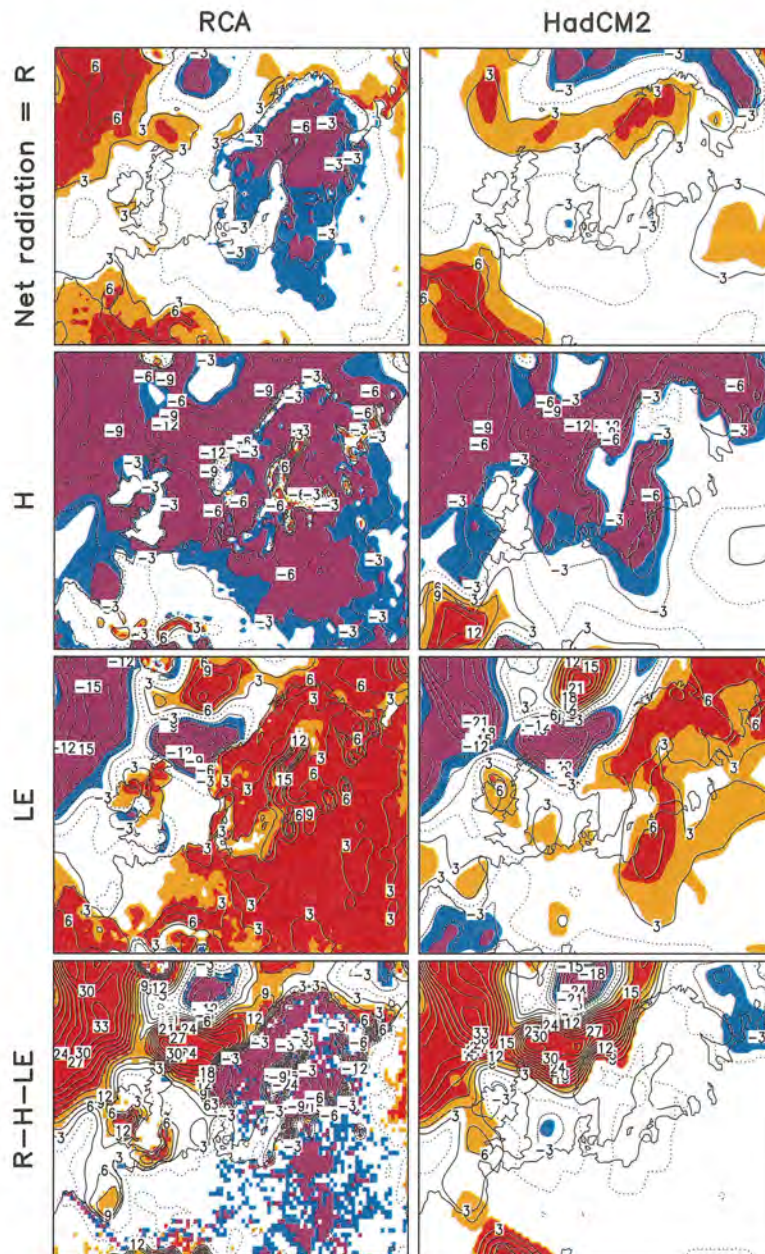


Figure 10. 10-year annual mean changes (scenario run – control run) in surface energy balance (Wm^{-2}) in RCA (left) and HadCM2 (right). From top to down: net radiation (R), sensible heat flux (H), latent heat flux (LE), and net surface energy balance (R-H-LE). A positive change in H (LE) indicates that surface loses more energy by sensible (latent) heat flux, whereas positive changes in R and G indicate that the surface gains more energy. Positive changes significant at the 90% (99%) level are shaded in orange (red), and negative changes significant at the 90% (99%) level in blue (violet).

Sensible heat flux from land surface to the atmosphere generally decreases in RCA, in particular in northern Europe. This appears to partly reflect a negative change in the surface radiation balance, which is most pronounced in winter when a decrease of cloud cover in northern Europe makes the net upward long-wave flux larger. In addition, the energy available for sensible heat flux is in RCA reduced by a widespread increase in

latent heat flux. The latter is consistent with the larger moisture holding capacity of the warmer air in the scenario run. In winter, decreases of snow cover (evaporation from snow is small in RCA) and lake ice also act to increase latent heat flux in RCA.

In HadCM2, the repartitioning between sensible and latent heat fluxes over land is less systematic than in RCA. In northern Europe the increase in annual mean latent heat flux in HadCM2 is similar to that in RCA, but in most of central Europe it is smaller and in Spain latent heat flux actually decreases in HadCM2. Apparently, evaporation in HadCM2 is more strongly constrained by drying of soil than in RCA (the difference between RCA and HadCM2 is largest in late summer and early spring when soil moisture is a minimum). Changes in sensible heat flux are also less systematic in HadCM2 than in RCA. Northern and central Europe are dominated by small (generally non-significant) decreases, but in Spain a marked increase in sensible heat flux occurs in HadCM2.

To summarize the findings of this and the previous subsection, the changes in radiation balance and surface energy balance have both similarities and differences between RCA and HadCM2. The latter seem to be associated with several model components, including soil and surface physics, cloud processes and treatment of CO₂ in the parameterization of long-wave radiation. The differences in the changes in radiation and surface energy balance have certainly connections with other differences in the climate response of the two models, but in this respect it is very difficult to separate the influence of individual factors.

3.8 Area mean statistics

The previous sections have compared the simulated changes (scenario run - control run) in several climate parameters in RCA and HadCM2. In this section the analysis is complemented with some area mean statistics. First, in Table 2, some annual area means are shown. In addition to the simulated changes, area means in the control runs are given for comparison. After this, Figs. 12 and 13 document the seasonal cycles of the simulated area mean changes in RCA and HadCM2. Table 2 gives area means for three regions: the whole RCA model domain excluding the boundary relaxation zones, 'Common land' and 'Common sea'. Common land (common sea) is defined as those RCA grid boxes in which the fraction of land in RCA and the bilinearly interpolated fraction of land in HadCM2 are both above (below) 50%. As the land-sea distributions in the two models differ, common land and common sea together cover only 93% of the RCA domain. Figs. 12 and 13 also include two smaller land areas, 'Northern Europe' and 'Sweden' (see Fig. 11).

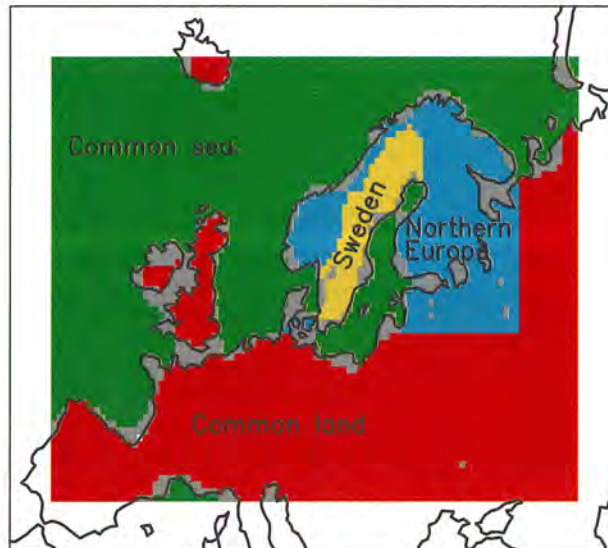


Figure 11. Areas used in Table 2 and in Figs. 12-13. 'Sweden' is a subdomain of 'Northern Europe' and 'Northern Europe' is a subdomain of 'Common land'.

Some of the observations one can make from the table and the two figures include the following:

- The annual and area mean temperatures in the control run and the changes from the control run to the scenario run are in the upper troposphere (300 hPa) very similar in the two models. In the mid- and lower troposphere and at 2 m, the average warming is slightly smaller in RCA, in particular over land areas which are slightly cooler in RCA even in the control run. The annual mean difference in land area mean surface air warming basically reflects smaller warming in RCA than in HadCM2 from May to October (see Fig. 12). The stronger warming in HadCM2 in summer has an apparent connection with changes in surface energy balance, which may reflect a positive soil moisture feedback (see below). The neglect of increased CO₂ in the RCA radiation scheme may also act to damp the warming in RCA.
- The area and annual mean precipitation increases somewhat more in RCA (9.8% in the whole domain) than in HadCM2 (8.0%) even in relative terms, and the absolute difference is larger because there is more precipitation in the RCA than in the HadCM2 control run. Over land, both models simulate a larger increase in convective than in large-scale precipitation, but over sea the fraction of convective precipitation decreases. The latter result reflects the relatively small increase in SSTs in northern North Atlantic.

Table 2. 10-year annual area means of different parameters in the RCA and HadCM2 (Had) control runs, and the changes from the control run to the scenario run. For definition of the areas see Fig. 11. The radiation fluxes (from SW_{net} , TOA to R_{net} , surface) are defined positive when directed downward, whereas H and LE are positive when directed upward.

		All (excl. boundaries)			Common sea			Common land		
		RCA	Had	R-H	RCA	Had	R-H	RCA	Had	R-H
T(300 hPa) (°C)	Control	-52.4	-52.5	0.1	-52.7	-52.8	0.1	-52.2	-52.2	0.0
	Change	3.25	3.24	0.01	3.03	3.05	-0.02	3.43	3.40	0.03
T(500 hPa) (°C)	Control	-26.1	-25.9	-0.2	-26.6	-26.4	-0.2	-25.6	-25.4	-0.2
	Change	3.64	3.83	-0.19	3.43	3.57	-0.14	3.79	4.02	-0.24
T(850 hPa) (°C)	Control	-0.8	-0.4	-0.5	-1.3	-0.9	-0.4	-0.4	0.1	-0.6
	Change	2.87	2.97	-0.10	2.67	2.69	-0.02	3.00	3.18	-0.17
T(2 m) (°C)	Control	6.0	6.4	-0.4	8.1	8.0	0.1	4.3	5.1	-0.7
	Change	2.83	2.92	-0.10	2.22	2.22	0.00	3.27	3.47	-0.21
Precipitation (P) (mm/year)	Control	923	847	76	1073	947	126	796	777	20
	Change	90 (9.8%)	68 (8.0%)	22 (1.8%)	84 (7.8%)	69 (7.2%)	15 (0.6%)	89 (11.2%)	64 (8.3%)	25 (2.9%)
Large-scale P (mm/year)	Control	546	426	120	491	440	52	596	416	180
	Change	74 (13.6%)	40 (9.3%)	34 (4.3%)	94 (19.2%)	57 (13.0%)	37 (6.2%)	57 (9.6%)	25 (6.1%)	32 (3.5%)
Convective P (mm/year)	Control	377	421	-44	582	508	74	200	360	-160
	Change	16 (4.3%)	28 (6.7%)	-12 (-2.4%)	-10 (-1.7%)	12 (2.3%)	-22 (-4.0%)	32 (15.9%)	39 (10.8%)	-7 (5.1%)
Evaporation (mm/year)	Control	503	582	-78	715	742	-27	338	458	-120
	Change	17 (3.5%)	2 (0.3%)	16 (3.2%)	-18 (-2.5%)	-28 (-3.8%)	11 (1.3%)	43 (12.7%)	22 (4.9%)	21 (7.8%)
Cloud cover (% of sky)	Control	67.6	72.1	-4.5	66.7	73.8	-7.1	68.6	70.8	-2.2
	Change	-1.4	0.0	-1.4	-0.6	0.2	-0.8	-2.1	-0.2	-1.9
Wind at 10 m (m/s)	Control	6.21	5.84	0.37	8.71	7.36	1.35	4.22	4.65	-0.43
	Change	0.08 (1.3%)	0.01 (0.2%)	0.07 (1.2%)	0.06 (0.7%)	-0.01 (-0.2%)	0.07 (0.9%)	0.08 (2.0%)	0.02 (0.5%)	0.06 (1.5%)
SW_{net} , TOA (W/m^2)	Control	139	146	-7	138	141	-4	140	150	-10
	Change	1.7	-0.4	2.1	0.7	-2.3	3.0	2.5	1.2	1.3
LW_{net} , TOA (W/m^2)	Control	-201	-214	13	-203	-213	10	-200	-215	16
	Change	-6.3	-0.5	-5.9	-4.8	0.5	-5.3	-7.6	-1.3	-6.3
R_{net} , TOA (W/m^2)	Control	-62	-68	6	-65	-72	7	-60	-65	5
	Change	-4.6	-0.9	-3.8	-4.1	-1.8	-2.3	-5.1	-0.1	-5.0
SW_{net} , surface (W/m^2)	Control	94	93	1	93	90	4	94	95	-1
	Change	0.3	-1.6	1.9	-0.5	-3.4	2.9	1.0	-0.1	1.1
LW_{net} , surface (W/m^2)	Control	-55	-43	-12	-62	-46	-16	-49	-42	-8
	Change	0.2	2.9	-2.7	2.4	4.0	-1.5	-1.5	2.0	-3.5
R_{net} , surface (W/m^2)	Control	39	49	-11	32	44	-12	45	54	-9
	Change	0.5	1.3	-0.8	1.9	0.6	1.3	-0.5	2.0	-2.5
H (W/m^2)	Control	20	19	1	25	22	3	17	18	-1
	Change	-4.2	-2.5	-1.7	-5.8	-5.7	-0.2	-3.0	0.1	-3.1
LE (W/m^2)	Control	40	46	-6	57	59	-2	27	37	-10
	Change	1.4	0.1	1.3	-1.4	-2.3	0.9	3.4	1.6	1.8

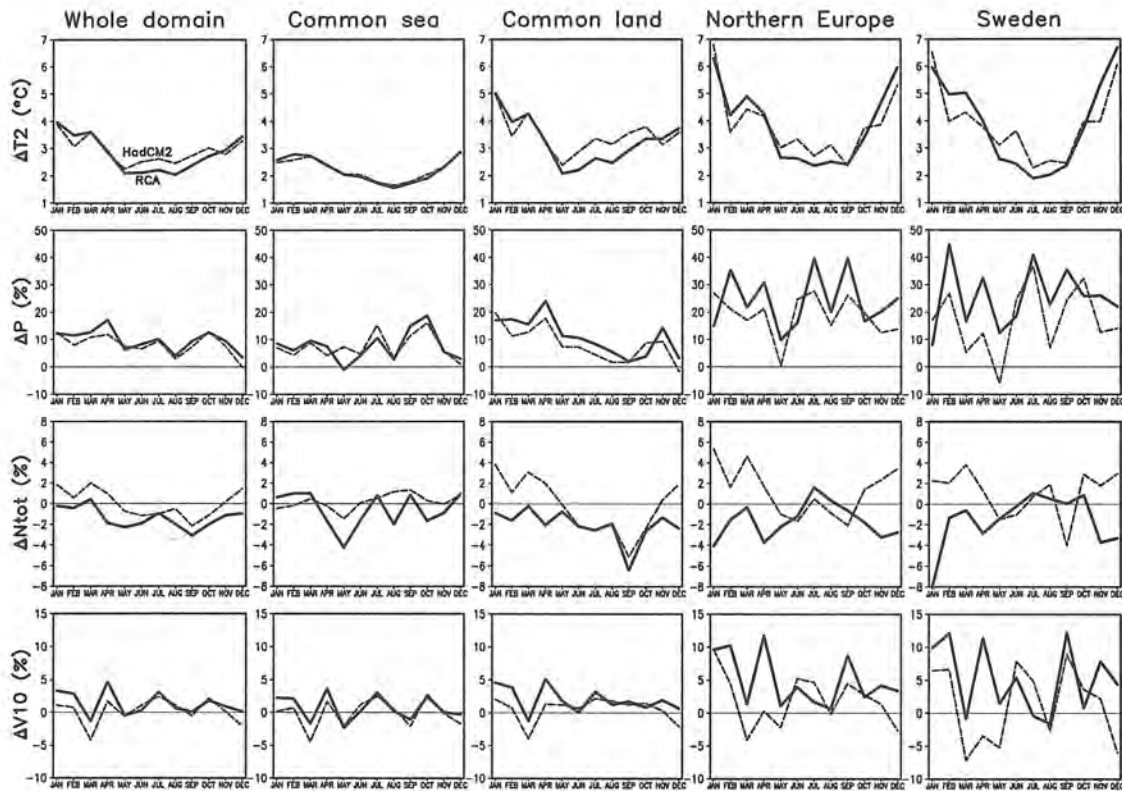


Figure 12. Simulated monthly and area mean changes in surface air temperature ($^{\circ}\text{C}$), precipitation (% of area mean in respective control run), total cloudiness (% of sky) and mean wind speed at 10 m height (% of area mean in respective control run) in RCA (thick solid lines) and HadCM2 (thin dashed lines).

- The larger increase in annual mean precipitation in RCA than in HadCM2 is consistent with a larger increase in evaporation over land and a smaller decrease in evaporation over sea. In both models, however, the increase in evaporation in the whole RCA domain is only a small fraction of the increase in precipitation. Thus, the increase in precipitation must be mainly associated with increased transport of water vapour from outside the RCA domain.
- Although the annual and area mean *changes* in the difference between precipitation and evaporation (P-E) are similar in RCA (73 mm/year) and HadCM2 (66 mm/year), there is a substantial intermodel difference in P-E in the control runs. Precipitation is larger but evaporation smaller in RCA than in HadCM2, giving a substantially larger area mean P-E in RCA (420 mm/year) than in HadCM2 (265 mm/year). These figures refer to the RCA domain without the boundary relaxation zones, but the intermodel difference in P-E is not sensitive to including these.

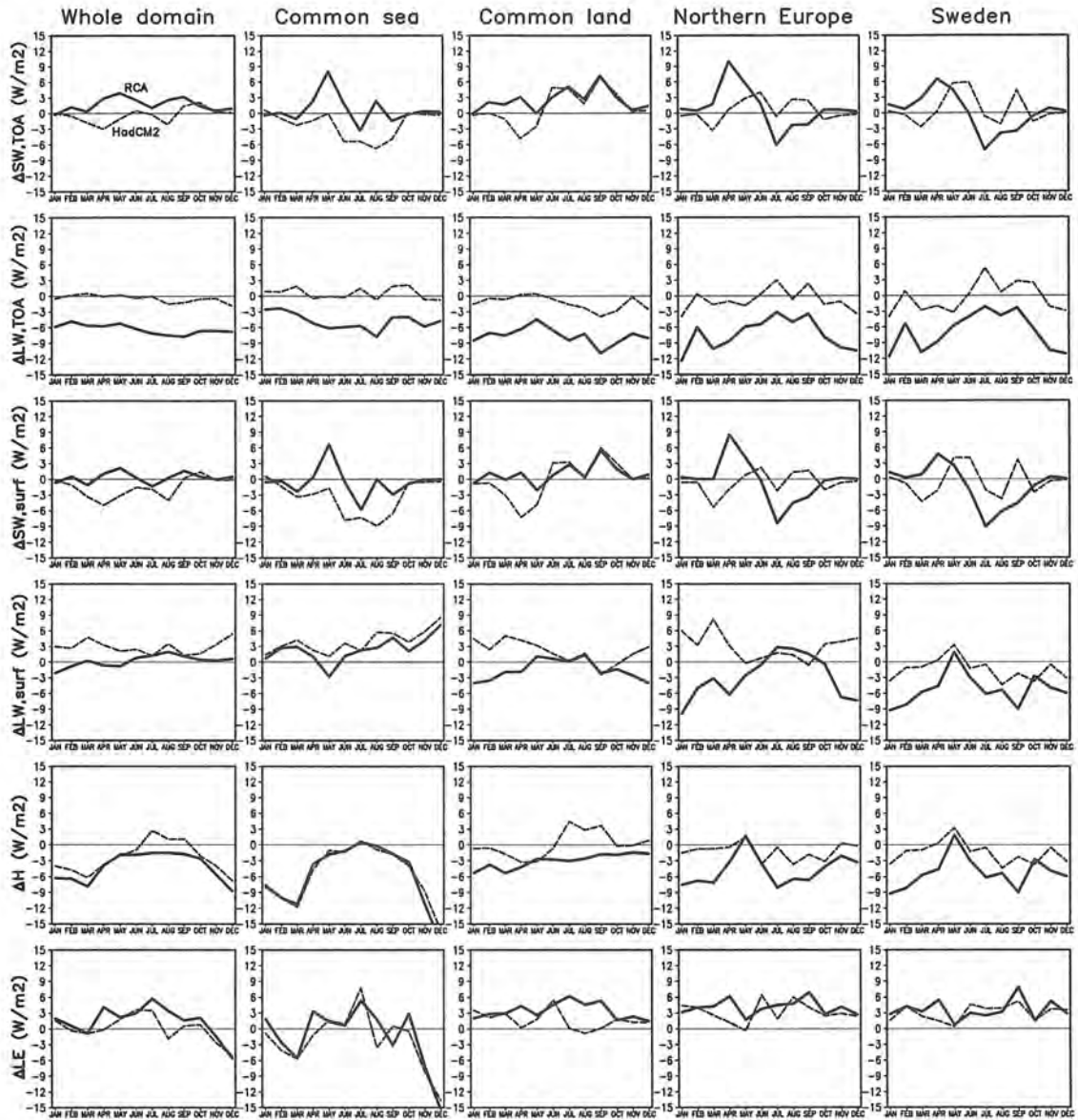


Figure 13. Simulated monthly and area mean changes (Wm^{-2}) in net short-wave (SW) and long-wave (LW) radiation at TOA and at surface, and in surface sensible heat flux (H) and latent heat flux (LE). The changes in RCA are shown with thick solid lines and those in HadCM2 with thin dashed lines. All radiation fluxes are defined positive toward the surface but H and LE are positive when directed from the surface toward the atmosphere.

- Annual and area mean total cloudiness in the control run is smaller in RCA than in HadCM2, in particular over sea. In the scenario run, the decrease in average cloud cover in RCA makes this difference even larger. As noted in Section 3.4 and shown by Fig. 12, the largest difference between the models in their simulated changes in cloudiness occurs in northern Europe in winter.
- Compared with the relatively large increase in mean wind speed at 10 m in RCA in northern Europe in winter, changes averaged over larger areas are much more modest in both models.

- The decrease in TOA long-wave radiation balance (i.e., increase in outgoing long-wave radiation) in RCA and the contrast with little change in HadCM2 are very systematic, present in the area means for all five areas in each individual month (Fig. 13). Many of the other area mean changes in the radiation budget components and the intermodel differences in them are surprisingly well correlated with changes in area mean total cloudiness (compare, for example, the monthly changes in mean cloudiness in Northern Europe in Fig. 12 with the changes in the net long-wave flux at the surface in Fig. 13).
- The radiation budgets in the RCA and HadCM2 control runs differ considerably. For example, the annual mean outgoing long-wave radiation averaged over the whole domain is 13 Wm^{-2} smaller in RCA than in HadCM2. Over a half of this difference remains even in the scenario run, in spite of the marked increase in outgoing long-wave radiation in RCA.
- Area mean sensible and latent heat fluxes over sea in RCA and HadCM2 are in fair agreement, regarding both the values in the control run and the simulated changes. Over land, RCA simulates a smaller annual and area mean latent heat flux in the control run but a larger increase from the control run to the scenario run than HadCM2. The difference in control run may be in part explained by the tendency of the RCA soil model to lose water through its lower boundary (see Rummukainen et al. 1998). The intermodel difference in the changes from the control run to the scenario run is largest in late summer and early autumn. In this season, RCA simulates a clear increase in land area mean evaporation but the change in HadCM2 is close to zero (see Fig. 13), which suggests that evaporation in the HadCM2 scenario run is more strongly constrained by drying of soil. The small change in latent heat flux in HadCM2 in late summer and early autumn is accompanied by an increase in land area mean sensible heat flux in this model in the same season, whereas RCA simulates an area mean decrease in sensible heat flux throughout the year. The increase in sensible heat flux in HadCM2 probably contributes to the larger surface air warming in this model in summer and autumn. These remarks refer to area means over all common land; in area means over northern Europe alone only some of the mentioned features are seen.
- With the 10-year averaging period used, the noise caused by internal climate variability can not be neglected. The problem becomes increasingly serious with increasing time resolution and decreasing averaging domain (see, for example, the monthly mean changes in Sweden mean precipitation or mean wind speed in Fig. 12).

4 Further aspects of climate change in RCA

4.1 Surface hydrology

After having compared the simulated changes in several variables in RCA and HadCM2, we study a few additional parameters in RCA. First, the changes (scenario run – control run) in annual mean net precipitation (P-E), surface runoff, and the difference between these two are shown in Fig. 14.

The changes in P-E are mostly dominated by changes in precipitation (which were shown in relative units in Fig. 5). In general, annual mean P-E increases in northern Europe, with varying changes in southern and eastern parts of the model domain. However, since evaporation increases over almost all land areas (see Fig. 10; an increase of 1 Wm^{-2} in latent heat flux indicates an increase of 13 mm per year in evaporation), the changes in P-E are less positive than those in P. As an interesting detail, the simulated change in P-E at the east coast of southern Sweden is marginally negative, despite a slight increase in precipitation.

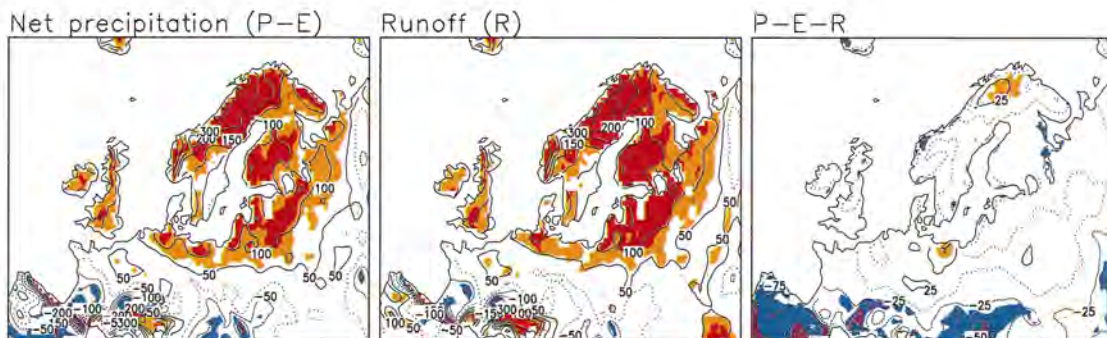


Figure 14. Simulated annual mean changes in RCA in net precipitation (P-E) and runoff (R), and the difference between these two (P-E-R). Contours at 0 (stippled) and ± 50 , ± 100 , ± 150 , ± 200 , ± 300 and ± 400 mm/year (P-E and R) or every 25 mm/year (P-E-R). Increases significant at the 90% (99%) level are shaded in orange (red), and decreases significant at the 90% (99%) level in blue (violet).

The changes in runoff are very similar to those in P-E. In nature, differences between these two would only arise from variations in the water storage of soil and snow cover, and the contribution of these variations to 10-year mean water budget should be negligible. However, as discussed by Rummukainen et al. (1998), the soil model used in the first version of RCA does not conserve water. Rather, relaxation towards deep-soil moisture contents inferred from the HadCM2 simulation led in the control run to substantial positive and negative values of P-E-R (in most of the model domain the 10-year mean P-E-R was positive, so that the sum of runoff and evaporation was smaller than precipitation). The similarity between the changes in P-E and R suggests that the nonconservativity of the soil model does not seriously distort the model's annual mean

hydrological response in northern and central Europe. The only larger area where the simulated change in P-E-R is substantial is southern Europe, where the change in runoff is less negative than that in P-E.

In northern Europe, runoff increases slightly in summer and autumn and more strongly in winter, but it decreases somewhat in Finland and northern Scandinavia in spring (not shown). Winter temperatures in the scenario run are substantially higher than in the control run, which enables a much larger part of the precipitation to fall in liquid form and makes melting of snow in the middle of winter more frequent. The smaller storage of water as snow increases runoff in winter but makes the spring peak in runoff due to snowmelt smaller (see also SWECLIM 1998).

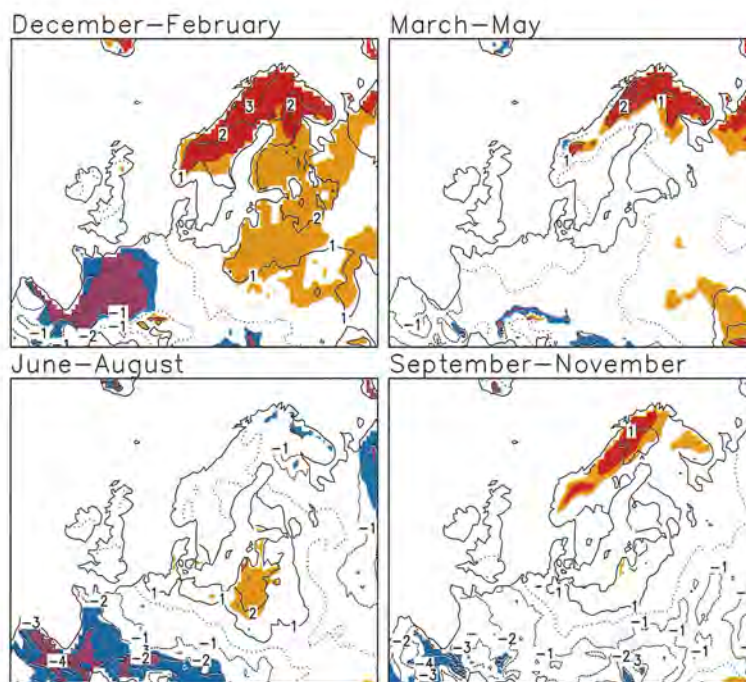


Figure 15. Simulated seasonal mean changes in top-layer soil moisture in RCA. Contours every 1 mm (the maximum water content of the layer is 20 mm). Positive changes significant at the 90% (99%) level are shaded in orange (red), and negative changes significant at the 90% (99%) level in blue (violet).

The simulated changes in soil moisture (Fig. 15) in RCA are typical of, or at least well within the scatter of other model results (e.g., Houghton et al. 1996; Räisänen 1997; 1998). In northern Europe, increased liquid precipitation and snowmelt in winter make the soil wetter in this season. In summer, the effects of increased precipitation and evaporation roughly compensate each other in northern Europe, so that there is little change in soil moisture (the earlier snowmelt may also act to reduce soil moisture in early summer). In the southern part of the model domain, soil becomes generally drier. Note that RCA predicts soil moisture in two layers and the results shown here are for the upper of these. However, seasonal mean changes in the moisture content of the lower layer are very similar.

4.2 Snow and ice

The warming in the RCA simulation is accompanied by a substantial decrease in snow (see Fig. 16). The length of the snow season (defined as the annual number of days when the water content of the snow pack exceeds 1 mm) decreases in northern Europe by roughly two months. Near the Norwegian coast and the coastlines of the Baltic Sea the change is locally even larger. Further southwest, where the snow season is short even in the control run, the absolute change is naturally smaller. One can also characterize the change by using geographical analogies. For example, the snow season in the scenario run in central Sweden and southwestern Finland is similar to that in Denmark in the control run, whereas the conditions of central Sweden in the control run retreat northeast to eastern Finland in the scenario run.

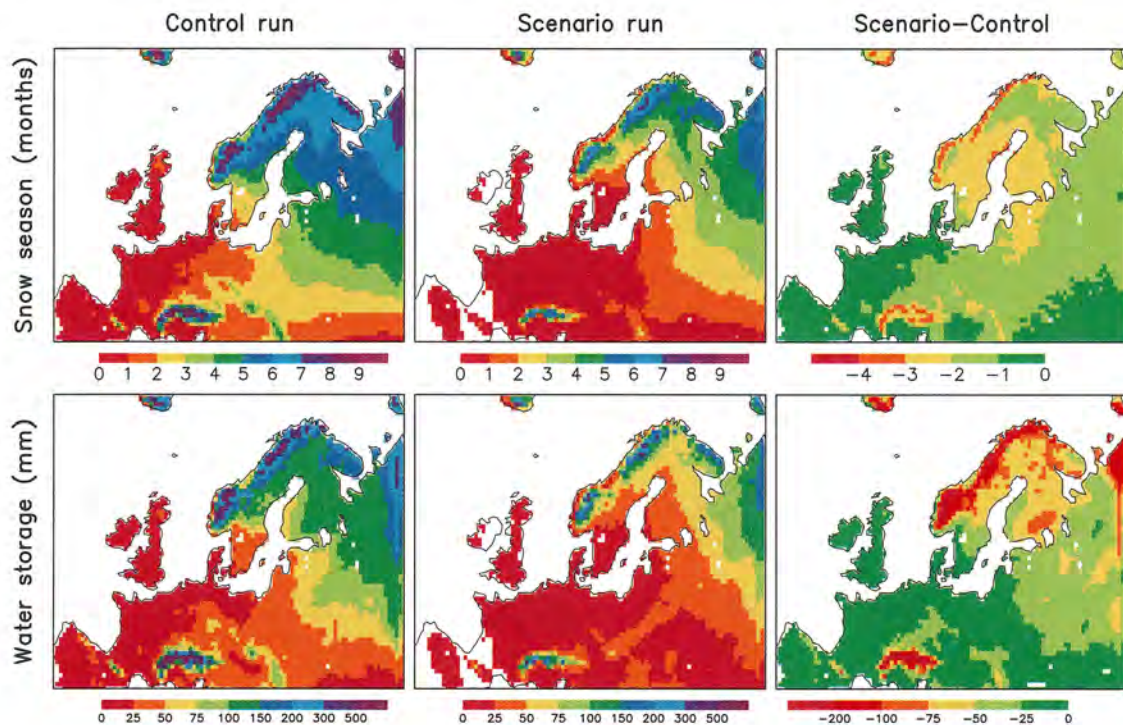


Figure 16. Average length of the snow season in months (above) and the 10-winter mean maximum water content of the snow pack in mm water (below) in the control run and in the scenario run, and the difference scenario-control.

In addition to staying on the ground a shorter period than in the control run, the snow pack in the scenario run never grows as thick (lower part of Fig. 16). Even in northern Scandinavia where winter precipitation increases by over 40%, the 10-year mean annual maximum water storage in snow decreases substantially. The increase in precipitation is overcompensated by the effects of the large warming: a larger part of the precipitation falls in liquid form, and melting episodes in winter become more frequent. In terms of geographical analogies, the changes in annual maximum snow water content are similar to those in the length of the snow season.

The existence of lake ice is, in the first version of RCA, inferred from soil temperatures. A similar method is applied to sea ice in the Baltic Sea and the White Sea (Rummukainen et al. 1998). Like air temperature, soil temperatures in the scenario run are several degrees higher than those in the control run, which directly translates to a much shorter ice season (Fig. 17). The shortening of lake ice period is similar to, or even larger than, that of the snow period. In parts of Sweden, for example, the 10-year mean change is over three months.

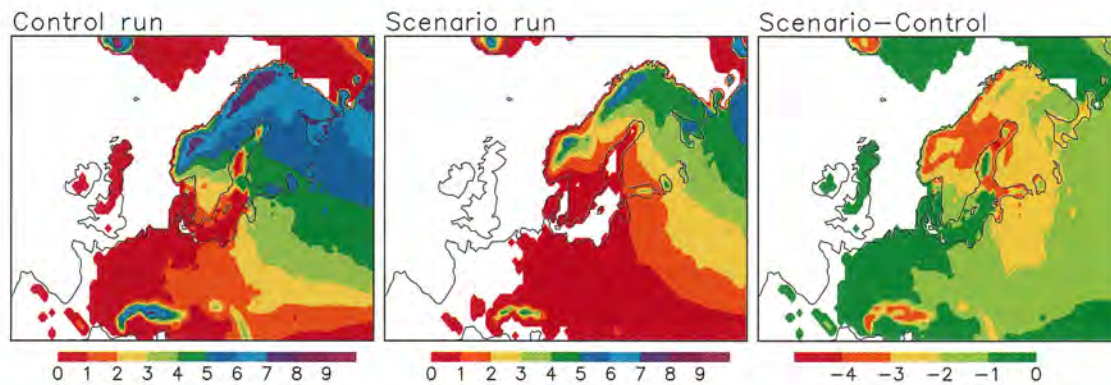


Figure 17. Average length of the ice season in months in the control run and in the scenario run, and the difference scenario-control.

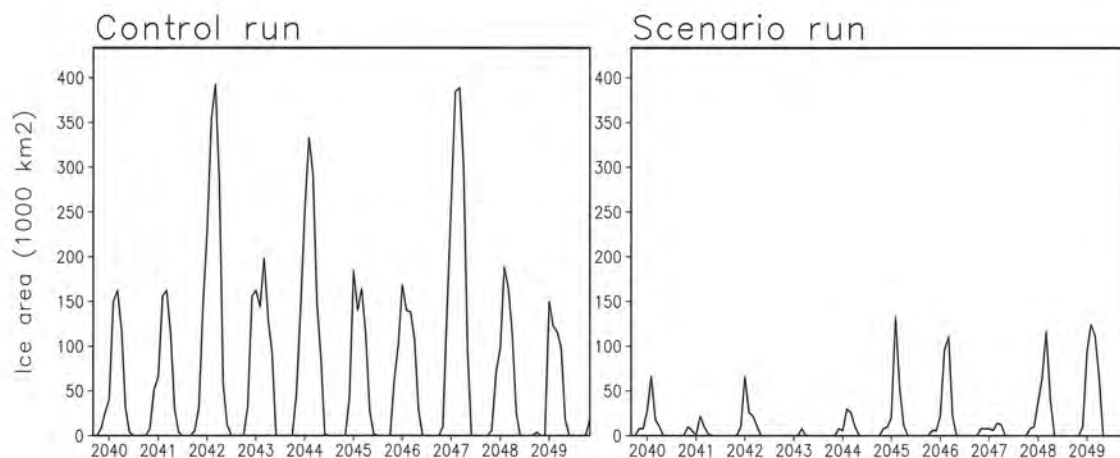


Figure 18. Area of Baltic Sea ice cover in the middle of each month in the control run and in the scenario run.

Ice cover in the Baltic Sea is also dramatically reduced. In the scenario run, ice never develops in Baltic Proper and most of the Bothnian Sea. The average length of the ice season exceeds one month only in the Gulf of Finland and in the extreme north of the Bothnian Bay. For another illustration of the change, Fig. 18 shows the total Baltic Sea ice area on the 15th of each individual month in the control and the scenario runs. Both runs exhibit a good deal of interannual variability, but the difference in overall ice

amount is striking. In the control run, the annual maximum ice area calculated from the mid-month values varies between 35% and 91% of the total Baltic Sea area of 433.000 km². In the scenario run, the range is from only 2% to 30%. For comparison, the observed range in 1720-1992 was from 12% to 100% (Seinä and Palosuo 1993; Omstedt and Cheng 1998).

Due to the crude way in which ice cover was treated in the first RCA simulations, the results concerning lake ice and sea ice are of a very preliminary nature. Because of the importance of ice cover for other aspects of winter climate, in particular surface air temperature, a more physically based treatment of ice is necessary in the next RCA simulations.

4.3 Variability of temperature and precipitation

The previous sections have only discussed the simulated climate changes in terms of seasonal and annual means. However, an enhanced greenhouse effect may also affect the variability of climate on different time scales, and for many practical applications changes in variability and extremes are at least as important as those in the mean state. This section shows some results associated with temperature and precipitation variability on short time scales (diurnal cycle and daily variations). Changes in variability on longer (such as interannual) time scales are difficult to infer from 10-year model simulations and are not discussed here.

Changes in the diurnal variability of surface air temperature are shown in Fig. 19 using two different definitions. *Diurnal temperature range* is the most commonly used parameter in this context and it is defined as the average difference between daily maximum and minimum temperatures. In addition, we calculate a *diurnal temperature amplitude*. This is obtained by computing, for each simulated month, the mean temperatures at 00, 06, 12 and 18 UTC separately, and by then fitting a single fourier harmonic to these. Diurnal temperature amplitude is the amplitude of this fourier harmonic multiplied by two. The two parameters differ in part because the average diurnal temperature cycle may not be completely described by a single harmonic. More importantly, however, the diurnal temperature range is affected by irregular day-to-day temperature fluctuations. This difference is essential in northern Europe in winter, when the small amount of solar radiation makes regular diurnal variability small but day-to-day temperature fluctuations are large. For example, a linear 15°C temperature change in 24 hours, which is not exceptional in northern Europe in winter, gives a diurnal range of 15°C that has nothing to do with the regular diurnal cycle.

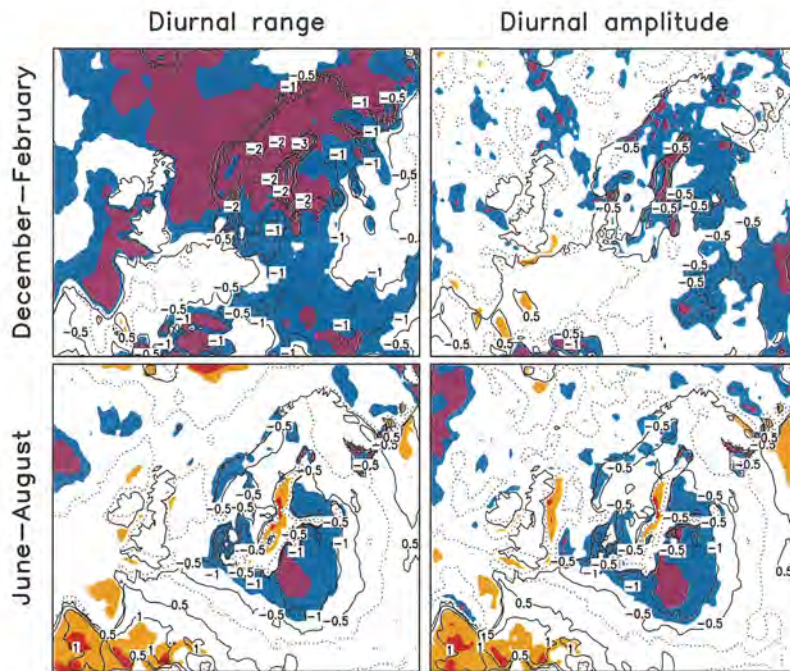


Figure 19. 10-year mean changes (scenario run – control run) in diurnal temperature range and diurnal temperature amplitude in RCA in December-February (above) and June-August (below). Contours at 0 (stippled) and ± 0.5 , ± 1 , ± 2 and $\pm 3^\circ\text{C}$. Increases significant at the 90% (99%) level are shaded in orange (red), and decreases significant at the 90% (99%) level in blue (violet).

The changes (control run – scenario run) of wintertime diurnal temperature range and temperature amplitude are in fact far from identical (see the upper part of Fig. 19). Both parameters generally decrease in northern Europe, but the decreases in diurnal temperature range are larger (even in relative terms, see Table 3) and of higher statistical significance than those in diurnal amplitude. This implies a small weakening of the regular diurnal temperature cycle but a larger decrease in irregular day-to-day temperature fluctuations. In summer, when regular day-night variability is larger and day-to-day temperature fluctuations are smaller, the two parameters give much more similar results. They are also in fair agreement in spring and autumn.

Mechanisms inducing changes in diurnal temperature variability can be quite complicated (e.g., Watterson et al. 1997). Factors that may be of importance for the present results include the following:

- Decreases in lake ice and Baltic Sea ice damp day-to-day temperature variability in winter at least in the Nordic region by allowing large fluxes of sensible and latent heat from water to air when air is cold.
- Decrease in snow may act to damp both day-to-day and day-night temperature differences. In the model as in nature, snow is a good insulator that reduces heat exchange between air and the ground. On the other hand, snow-free surface has a lower albedo than snow-covered surface, which acting alone would make day-night

temperature difference larger when snow decreases (i.e., a decrease in albedo should increase temperature more during daylight hours than at night). However, it seems that the net effect of snow in the model is indeed to amplify day-night temperature differences. Largest reductions in diurnal temperature *amplitude* from the scenario run to the control run, locally over 1°C, occur in northern and eastern parts of the model domain in spring and have an apparent connection with reduced snow cover.

- In summer, the patterns of change in diurnal temperature amplitude indicate a negative correlation with changes in total cloudiness (Fig. 6) and soil moisture (Fig. 15). Reduced cloud cover acts to increase diurnal temperature amplitude by both increasing daytime temperatures and reducing night temperatures. Drying of soil, in turn, tends to inhibit evaporation and thus favours a larger daytime sensible heat flux, which increases daytime temperatures near the ground. In autumn as well (not shown), increased diurnal amplitude in the southern part of the model domain coincides with reduced soil moisture.

As averaged over all land areas in the RCA domain, the simulated diurnal temperature range decreases markedly in winter and spring but there is little systematic change in summer and autumn. Diurnal temperature amplitude shows, in absolute terms, a substantial decrease only in spring (see Table 3).

Table 3. 10-year seasonal and annual mean changes in diurnal range and diurnal amplitude of surface air temperature (in °C and in per cent of the area mean in the control run), averaged over land grid boxes in the RCA domain excluding the boundary zones.

	DJF	MAM	JJA	SON	Annual
Diurnal range	-0.85 (-13%)	-0.76 (-10%)	-0.03 (-0%)	-0.01 (-0%)	-0.41 (-5%)
Diurnal amplitude	-0.23 (-8%)	-0.56 (-9%)	-0.04 (-0%)	0.18 (+4%)	-0.13 (-3%)

The absolute annual temperature range (10-year mean difference of annual absolute maximum and minimum temperatures) decreases in most of the model domain (Fig. 20). In the Nordic region, in particular, the increase in annual minimum temperature is substantially larger than the increase in annual maximum. The latter is, in most of Finland, Sweden and Norway, only 1-3°C, but the former exceeds 12°C in central Sweden and along the coasts of the Baltic Sea. Evidently, this huge increase in winter minimum temperatures is affected by the decrease in Baltic Sea ice cover. In southern and central Sweden, for example, it makes a large difference in temperature whether the coldest air masses approaching from east or northeast have to cross an ice-free Baltic Sea or not. Naturally, in addition, a cold air mass is less cold in the scenario run than in the control run, even before being heated over open water. Finally, it should be noted that the coldest winter temperatures in the control run are in the Nordic region somewhat below those observed (Rummukainen et al. 1998), even though winter mean

temperatures are very reasonable. This adds some difficulty in the interpretation of the large increase in the absolute minima.

The simulated increase in winter minimum temperatures is largest around the Baltic Sea, but it is several degrees larger than the increase in winter mean temperature in central Europe as well. In addition to changes in ice cover and air mass characteristics, reduced snow cover most likely plays a role. The increase in absolute summer maximum temperatures is also in most of the model domain slightly larger than the increase in summer mean temperature, but the Nordic region is an exception. It is important to remember, however, that the brevity (10 years) of the simulation period is a larger problem in quantifying changes in annual extremes than it is in the case of mean conditions.

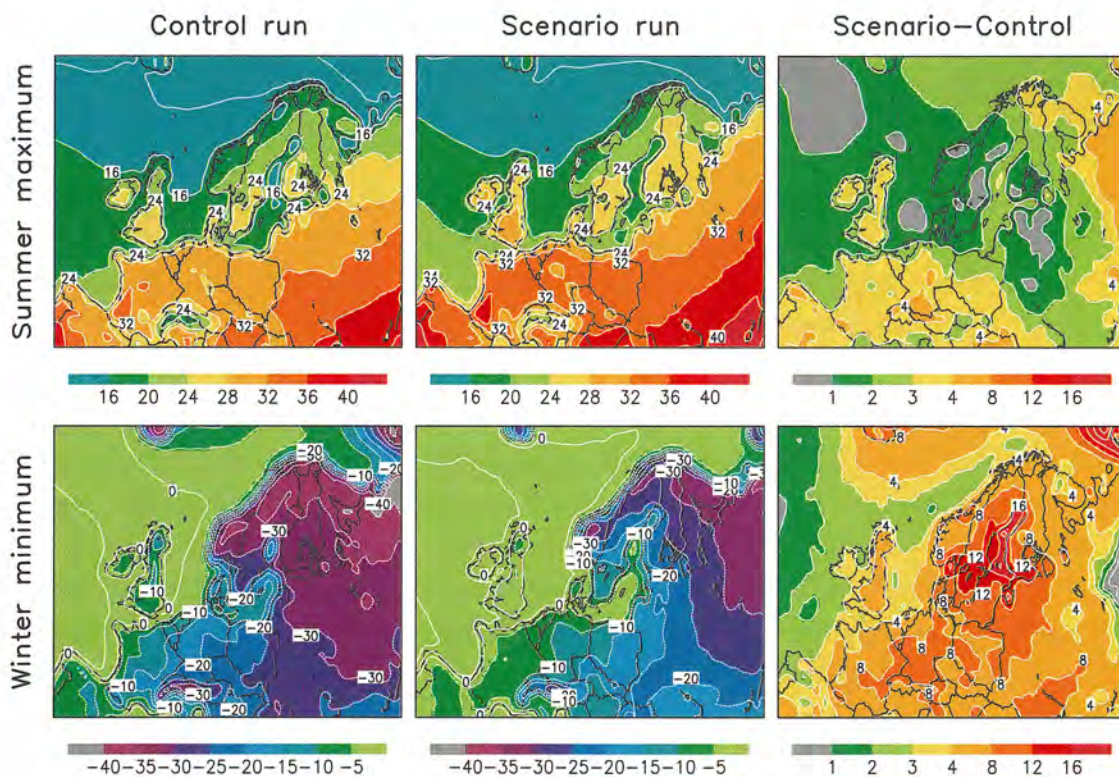


Figure 20. 10-year mean values of absolute annual maximum (above) and minimum temperature (below) in the control run and in the scenario run, and the difference scenario-control.

A simple and commonly used indicator of daily precipitation variability is the number of days when precipitation exceeds a selected threshold. Fig. 21 shows the changes (scenario run – control run) in the exceedence frequency of three different thresholds. For all of these, the geographical pattern of change resembles the change in annual mean precipitation (Fig. 5), with the most positive (negative) changes in northern Europe (in the southwestern part of the model domain). However, taking the model area as a whole, positive changes become more and more dominating with increasing

threshold. Increases in the number of days with at least slight precipitation (>0.1 mm) in the northern part of the model domain are balanced by decreases in southwest, but this is not the case with the thresholds 1.0 mm and 10 mm. While the absolute exceedence frequency of a daily precipitation of 1.0 mm increases generally more than that of 10 mm, the relative changes are larger in the latter. In parts of northern Sweden and Finland, the number of days with 10 mm or more of precipitation doubles in the scenario run.

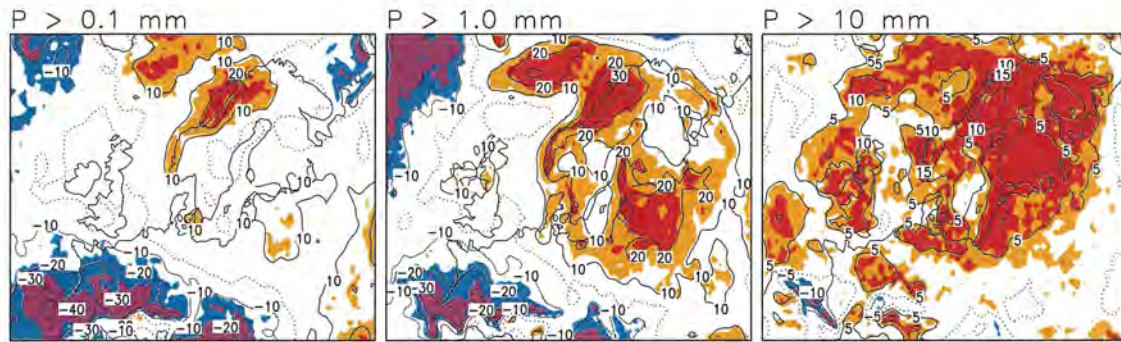


Figure 21. 10-year mean change (scenario run – control run) in the annual number of days with precipitation exceeding 0.1 mm (contours every 10 d), 1.0 mm (every 10 d) and 10 mm (every 5 d). Increases significant at the 90% (99%) level are shaded in orange (red), and decreases significant at the 90% (99%) level in blue (violet).

Statistics averaged over all land grid boxes in the RCA domain are shown in Table 4, using a slightly finer classification of daily precipitation totals. The area mean change in the number of dry days (<0.1 mm) is marginally positive. But, in wet days, the amount of precipitation is typically larger in the scenario run than in the control run (thus a slight decrease in the number of days with 0.1-5 mm of precipitation and an increase in the number of days with at least 5 mm of precipitation). The relative difference between the two frequency distributions is largest in the highest class (>20 mm/day). However, this does not necessarily indicate that the mechanism causing the change in the frequency distribution would be specific to heavy precipitation events (such as a large increase in the number of violent convective storms). As demonstrated by Frei et al. (1998), a similar change in frequency distribution might be obtained by simply multiplying each daily precipitation in the control simulation with a constant factor. An indication of that the shape of the frequency distribution remains, except for an overall shift towards larger amounts, more or less the same, is obtained by studying the changes in the 10-year means of annual maximum daily precipitation. These have a noisy geographical pattern (not shown), but in the land area mean, the increase is only 13%. This is just slightly larger than the change in land area mean total annual precipitation (11%).

Table 4. *Statistics of daily precipitation variability in the RCA control and scenario run, averaged over all land grid boxes excluding the boundaries. The first six columns give the average annual number of days with different precipitation amounts, and the last column the 10-year mean of largest annual one-day precipitation.*

	< 0.1 mm	0.1-1 mm	1-5 mm	5-10 mm	10-20 mm	> 20 mm	Pmax
Scenario	111 d	103 d	97 d	32 d	17 d	5.3 d	38.1 mm
Control	110 d	109 d	98 d	30 d	14 d	4.0 d	33.6 mm
Scenario-Control	1 d (1%)	-6 d (-6%)	-1 d (-1%)	2 d (6%)	3 d (17%)	1.3 d (33%)	4.5 mm (13%)

Finally, one should note that the frequency distribution of daily precipitation in the RCA control run is somewhat different from that observed, at least in Sweden (Rummukainen et al. 1998). Days with slight (heavy) precipitation are too common (rare) in the model. However, this is probably less important for the qualitative than the quantitative aspects of the present results.

5 Statistical significance of simulated climate change: a summary

Many of the maps presented in this report have included an indication of the statistical significance of the simulated climate changes. In some cases, there have been wide areas in which the statistical significance is high, which suggests that these results would have remained at least qualitatively similar even if a longer simulation had been performed. In other cases, areas of high statistical significance have been much less common. The *t* test results for a selection of variables are summarized in Table 5 by using the fractional area in which the changes were found to be significant. Some general comments:

- Seasonal and annual mean changes (increases) in surface air temperature have a high statistical significance almost everywhere. As the interannual variability of extremes is larger than that of mean conditions, changes (increases) in annual maximum and minimum temperatures are somewhat more commonly nonsignificant than the change in mean temperature. Still, even they have in most areas a reasonably high statistical significance. This also holds for the changes in snow and ice conditions (decrease of snow and ice), which more or less directly follow from the warming. Increases in outgoing long-wave radiation are also highly significant (in particular in annual mean), which reflects, most likely, the neglect of increased CO₂ in the radiation code.
- Annual mean changes in latent heat flux and sensible heat flux are also statistically significant in most areas. Over the northern North Atlantic, both generally decrease because the sea surface warms less than the overlaying air. Over land, the larger moisture holding capacity of warmer air allows the latent heat flux to increase, which reduces the energy available for sensible heat flux.

Table 5. *Percentage of areas in which the simulated climate changes (differences between the RCA scenario and control runs) are according to the t test statistically significant. In each table cell, the first number gives the proportion of changes significant at the 90% level and the second (in parentheses) the proportion of changes significant at the 99% level. The computation includes in most cases the whole model domain without the boundary relaxation zones ('All'), but only land areas when the parameter is undefined (soil moisture, surface runoff, snow and lake ice conditions) or uninteresting (diurnal variability of $T(2m)$) over sea. In addition, grid boxes that are totally snow- and ice-free in both the control and the scenario run are ignored in calculations related to ice and snow. P24 = one-day precipitation.*

			DJF	MAM	JJA	SON	Annual
Time Mean Surface Climate	T(2m)	All	99 (90)	100 (98)	100 (90)	99 (95)	100 (99)
	Precipitation	All	31 (13)	30 (5)	25 (7)	32 (8)	52 (28)
	Total cloudiness	All	44 (19)	16 (2)	19 (4)	29 (10)	40 (15)
	Mean wind speed	All	25 (8)	17 (4)	8 (0)	12 (1)	37 (14)
	Top-layer soil moisture	Land	51 (19)	18 (8)	21 (4)	11 (3)	42 (17)
	Surface runoff	Land	46 (28)	16 (2)	24 (5)	10 (0)	45 (21)
Atmospheric Circulation	Sea level pressure	All	34 (6)	50 (9)	19 (0)	11 (0)	68 (29)
	U(300 hPa)	All	32 (6)	27 (0)	13 (0)	18 (0)	33 (5)
Radiation and heat fluxes	SWnet, TOA	All	33 (15)	18 (6)	20 (6)	25 (8)	22 (8)
	LWnet, TOA	All	64 (43)	69 (42)	76 (43)	87 (55)	98 (93)
	SWnet, surface	All	31 (11)	14 (4)	22 (4)	23 (7)	15 (4)
	LWnet, surface	All	66 (45)	22 (7)	29 (4)	40 (10)	58 (35)
	Sensible heat flux	All	67 (34)	48 (16)	32 (14)	44 (10)	76 (54)
	Latent heat flux	All	53 (24)	55 (28)	61 (24)	59 (30)	78 (63)
Snow and ice	Length of snow season	Land					94 (84)
	Largest snow depth	Land					79 (43)
	Length of lake ice season	Land					94 (60)
Variability	Diurnal range of T(2m)	Land	51 (19)	51 (25)	24 (4)	36 (14)	56 (31)
	Diurnal amplitude of T(2m)	Land	31 (4)	39 (12)	26 (4)	25 (5)	44 (17)
	Annual maximum T(2m)	All					82 (51)
	Annual minimum T(2m)	All					95 (75)
	Days with P24 >0.1 mm	All					27 (9)
	Days with P24 >10 mm	All					54 (26)
	Annual maximum P24	All					23 (4)

- The changes in the other variables listed in Table 5 are less frequently significant, although the variation from case to case is large. With several parameters, the annual mean change is more commonly significant than the change in any individual season. This happens when the changes in different seasons tend to be to the same direction. For example, precipitation in northern Europe increases in all seasons with only local exceptions, but the changes in individual seasons have lower statistical significance than the annual mean change because the interannual variability of seasonal means is larger than that of annual means.
- The t test applied in the present study neglects interannual autocorrelation of unforced climate variability and assumes that these unforced variations follow a normal distribution. Both of these assumptions should be reasonably well justified

for most of the parameters studied here, but in some cases they may be violated. For example, interannual autocorrelation of surface air temperature over the Atlantic Ocean might not be negligible, and annual extremes probably follow the normal distribution less well than seasonal and annual means.

- Even if the assumptions underlying the t test are not violated, some 'significant' changes will emerge just by chance. In the absence of external forcing, this proportion would be – on the average – 10% (1%) for changes significant at the 90% (99%) level. Thus, for example, when the differences between the scenario run and the control run are significant at the 90% level in 20% of all grid boxes, about half of these significant differences are statistically just noise. Table 5 shows several cases in which the fraction of significant changes is even smaller. The problem is in relative terms less severe with changes significant at the 99% level, because such changes are in only a few cases a full 10 times more rare than changes significant at the 90% level. However, the absolute proportion of changes significant at the 99% level is in several cases small.
- The statistics in Table 5 refer to the significance of local (grid box scale) changes. Changes in climatic means over wider areas are generally expected to have better statistical significance. Some insight into how the effects of internal variability depend on the spatial scale may be gained from Figs. 12 and 13, in which irregular month-to-month variations grow larger with decreasing averaging domain.
- When climate changes are small compared with internal variability, they are likely to be of limited practical importance. Therefore, from a practical point of view, lack of statistically significant changes may also be an important result. However, changes that are small enough to be masked by internal variability during a single decade might still stand out clearly in longer-term statistics and might therefore be of importance for activities with a long time scale, such as forestry.
- Considering that the RCA simulations were only 10 years long, there are plenty of statistically significant changes in many variables. This is due to the strong forcing, a 150% increase in CO₂, applied in the driving global model. The disadvantage of this strong forcing is that the timing of the resulting climate change scenario is far into the future, rather 100 than 50 years from the present. However, assuming that anthropogenic climate changes grow roughly linearly with time, the 'signal' in a simulation presenting conditions 50 years from present would have had a 50% smaller amplitude. To get a similar 50% reduction in the amplitude of internal variability, a 40-year rather than a 10-year averaging period would have been needed.
- A reasonably high statistical significance is a necessary but not a sufficient condition for obtaining a 'reliable' estimate of the climatic impact of increased greenhouse gases. If the model is poor, the signal can be completely wrong even when it is well discernible from the noise.

Another question of interest is if the climate changes simulated by RCA are in a statistically significant manner *different* from the changes in the driving HadCM2

model⁶. Testing this leads to a slightly different strategy for variables whose changes are expressed in absolute terms (such as surface air temperature) than for those whose changes are more meaningfully given in relative units (such as precipitation). For the former group of variables, we simply calculated the differences between the RCA and HadCM2 simulated seasonal and annual means for each individual year in the control and scenario runs. Then, the *t* test was applied to study if the 10-year mean RCA-HadCM2 differences in the scenario run were significantly different from the 10-year mean differences in the control run.

For variables like precipitation, the most interesting question is not if the absolute differences between the two models are different between the scenario run and the control run but rather if there is a significant change in the ratio between the climatic means in RCA and HadCM2. To test this, the HadCM2 simulated seasonal and annual values of (for example) precipitation in each individual year of the control and scenario run were first multiplied by the ratio between the corresponding 10-year means in the RCA and HadCM2 control runs. Then, the *t* test was used to address if the scenario run mean deviation between the RCA simulated values and the scaled HadCM2 values was large enough to be statistically significant against the interannual variability of this deviation in the control and scenario runs. The *t* values given by this method are always zero when the 10-year mean relative changes in the two models are the same.

Results of these significance tests for four variables are given in Table 6. The intermodel differences in temperature change are at least weakly (at the 90% level) significant in a moderately large area in all seasons. By contrast, significant differences in precipitation changes are, excluding winter and annual mean, just slightly more common than one would expect to obtain by chance. On the other hand, the intermodel differences in changes in total cloudiness and 10 m mean wind speed are in some seasons more commonly significant than the changes as such in either of RCA (Table 5) or HadCM2 (not shown)! This is not as paradoxical as it might seem, because the interannual variations of these variables in RCA and HadCM2 are strongly correlated in both the control and scenario runs. Therefore, the variability of the RCA-HadCM2 differences is smaller than the variability in either of the two models individually. Nevertheless, when the differences between the climate changes in RCA and HadCM2 are statistically significant, they also tend to be large in absolute terms. This is the case, for example, with wintertime changes in mean wind speed and total cloudiness. A major factor behind the intermodel differences in these particular cases may be different feedbacks associated with reduced snow and ice cover.

⁶ By the HadCM2 simulated values we mean the values interpolated bilinearly to the RCA grid.

Table 6. Percentage of areas in which the simulated climate changes in RCA are significantly different from those in HadCM2 (see text). In each table cell, the first number gives the proportion of differences significant at the 90% level and the second (in parentheses) the proportion of differences significant at the 99% level. The computation includes the whole RCA model domain without the boundary relaxation zones.

	DJF	MAM	JJA	SON	Annual
T2	31 (10)	35 (11)	43 (10)	31 (12)	51 (25)
Precipitation	20 (5)	14 (2)	12 (1)	12 (1)	22 (6)
Total cloudiness	47 (20)	25 (6)	18 (4)	19 (4)	49 (20)
Mean wind speed	30 (11)	20 (6)	9 (0)	14 (2)	30 (13)

As an example, the RCA-HadCM2 differences in changes of annual mean surface air temperature and precipitation and the significance of these differences are shown in Fig. 22.

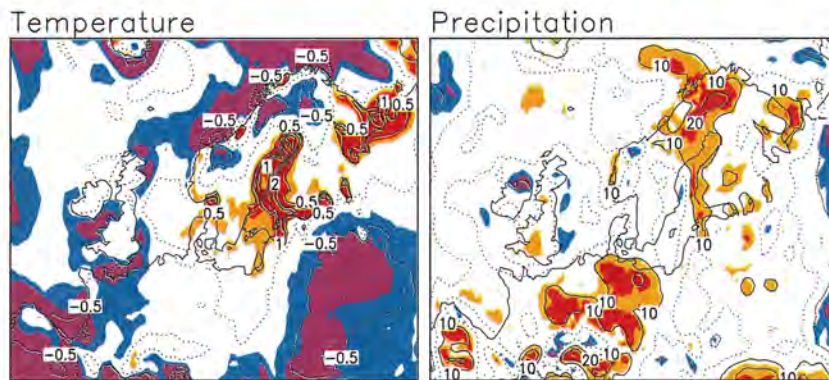


Figure 22. Difference RCA-HadCM2 in changes of annual mean surface air temperature (°C) and precipitation (per cent of 10-year mean in the control run). Areas where the change is at the 90% (99%) significance level more positive in RCA than in HadCM2 are shaded in orange (red), and areas where the change is at the 90% (99%) significance level more negative in RCA than in HadCM2 in blue (violet).

6 Climate change in HadCM2 – comparison of the 10-year time slice with longer model runs

As noted in Section 2.3, the 10-year HadCM2 runs used for obtaining the boundary conditions for RCA are partial reruns (‘time slices’) of much longer HadCM2 integrations. Comparison between the 10-year time slices and the original longer runs provides a concrete possibility to estimate how much, and to which direction, the climate changes inferred from these time slices deviate from the longer-term behaviour of the model. To the extent that the 10-year mean climate changes in RCA are similar to those in HadCM2 (as is the case, for example, with the general features of temperature and precipitation change), such comparison also indicates how a longer integration period would have altered the RCA results.

We define the long-term mean HadCM2 control climate as a 240-year mean (model years 1860-2099) in the original control run described by Johns et al. (1997). This flux-corrected control run is remarkably stable, with virtually no drift in global mean surface air temperature (Johns et al. 1997). There do not appear to be any significant regional trends in northern Europe either. In the transient HadCM2 run with gradually increased CO₂, climate naturally changes with time, but at least as far as the global mean surface air temperature is considered, the change is very close to linear in time after about 1980 (see Fig. 2 of Mitchell and Johns 1997). We define the long-term mean HadCM2 'scenario' climate as the 110-year mean 1990-2099 in the original greenhouse run, adding five decades to both sides of the period 2039-2049. The difference in global mean surface air temperature between the 110-year scenario run mean and the 240-year control run mean is 2.60°C. This is, with two decimals, the same as the temperature difference between the 10-year repeated scenario and control runs used for the RCA downscaling experiment.

How surface air temperature and precipitation vary from decade to decade in the original control and scenario runs in the Nordic region is illustrated in Fig. 23 using area means over the 25 HadCM2 land grid boxes at least partly within the boundaries of Finland, Sweden, Norway and Denmark (see upper left panel in Fig. 24). In the control run, both temperature and precipitation hover irregularly around the 240-year mean, being positively correlated with each other. In the scenario run, both gradually increase although the rising trend is occasionally interrupted by interdecadal fluctuations. The scenario run is substantially warmer than the control run already in the end of the 20th century, presumably because this run neglected the cooling effect of sulphate aerosols and because the equivalent CO₂ content in the control run is representative of preindustrial rather than present conditions.

Also shown in Fig. 23 are the 10-year (December 2039 – November 2049) means of temperature and precipitation in the repeated control and scenario runs used at Rossby Centre. The temperature in the control run time slice is very close to the 240-year mean, in fact closer than it was in the same decade in the original control run (which was somewhat cold). Control time slice precipitation is also close, although slightly below, the long-term mean. However, the scenario run time slice appears to be somewhat ahead of its time in that both temperature and precipitation exceed the 110-year mean in the original scenario run. The difference in temperature is 0.58°C (1.3 times the interdecadal standard deviation of temperature in the 240-year control run) and that in precipitation 2.9% of the 240-year control run mean (1.2 standard deviations). These differences are not negligible, although they are within the normal interdecadal variability of HadCM2.

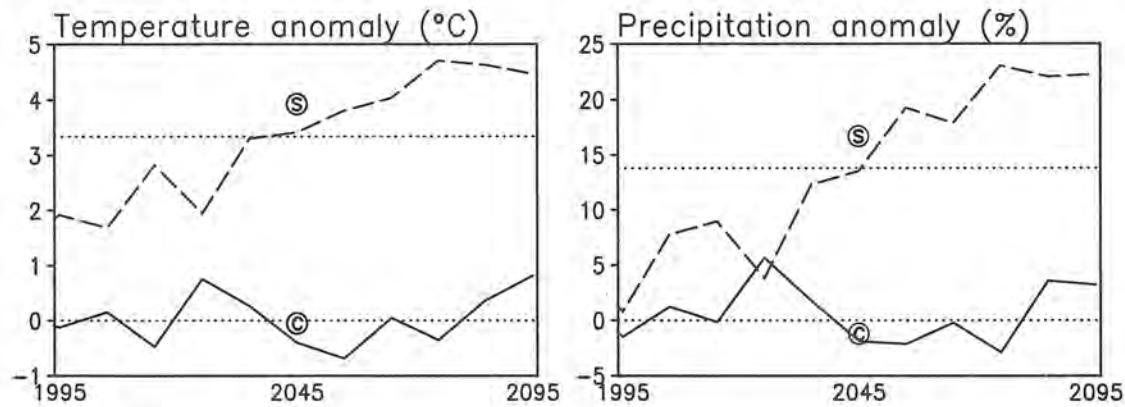


Figure 23. Decadal mean anomalies (differences from 240-year mean in the original control run) of Nordic land area mean surface air temperature (left) and precipitation (right) in HadCM2. The solid lines show the decadal anomalies for the original HadCM2 control run and the dashed lines those for the original scenario run between 1990 and 2099. The circled letters 'C' and 'S' indicate the anomalies for the repeated control and scenario runs, respectively. The two dotted lines show the mean anomalies for the original control run in 1860-2099 (by definition 0) and the original scenario run in 1990-2099.

Table 7. Seasonal and annual area means of surface air temperature and precipitation in the Nordic land area. 'Long run' refers to time means in the original control (1860-2099) and scenario runs (1990-2099), and 'time slice' to the 10-year means (2039-2049) used in the RCA experiment. The differences between the time slice means and the long run means are given in parentheses.

		Area mean (control)		Area mean (scenario)		Scenario – Control	
		Long run	Time slice	Long run	Time slice	Long run	Time slice
Temperature (°C)	DJF	-8.72	-8.70 (0.02)	-3.86	-3.04 (0.82)	4.86	5.66 (0.80)
	MAM	-0.66	-0.81 (-0.15)	2.65	3.11 (0.46)	3.31	3.92 (0.61)
	JJA	10.11	10.10 (-0.01)	12.29	12.92 (0.63)	2.19	2.83 (0.64)
	SON	1.82	1.77 (-0.05)	4.82	5.25 (0.43)	3.00	3.48 (0.48)
	ANN	0.64	0.59 (-0.05)	3.98	4.56 (0.58)	3.34	3.97 (0.63)
Precipitation (mm)	DJF	203	206 (3)	236	243 (7)	16.2%	18.1% (1.9%)
	MAM	187	187 (0)	208	205 (-3)	11.2%	9.5% (-1.7%)
	JJA	248	239 (-9)	273	288 (15)	9.9%	20.7% (10.8%)
	SON	248	244 (-4)	292	298 (6)	17.6%	22.2% (4.6%)
	ANN	886	875 (-11)	1008	1034 (26)	13.8%	18.1% (4.3%)

The Nordic land area mean temperature in the 10-year control time slice is close to the 240-year mean in the original control run and the mean for the 10-year scenario time slice somewhat above the 110-year mean in the original scenario run in all seasons (Table 7). The differences in area mean precipitation between the 10-year runs and the longer runs are largest in summer. Summer precipitation in the 10-year control time slice is 4% below the 240-year mean, whereas summer precipitation in the 10-year scenario time slice exceeds the 110-year scenario mean by almost 6%. As a result, the

difference in summer precipitation between the 10-year scenario and control runs is twice as large as the difference between the longer scenario and control runs.

Various difference maps related to the control and scenario run means of surface air temperature in the 10-year time slice and in the original longer experiment are shown in Fig. 24. Similar sets of maps for precipitation and sea level pressure are given in Figs. 25 and 26. For each variable and season, the first map gives the climate change calculated as the difference between the 10-year scenario and control runs, and the second the change obtained by using the 110-year scenario run mean and the 240-year control run mean. The third map shows the difference between the 10-year mean change and the longer-term-mean change, and the last two the differences between the 10-year time slice and the longer runs for control and scenario separately. These maps will not be discussed in detail but a few remarks are useful:

- The larger temperature difference in northern Europe between the 10-year scenario and control runs, as compared with the difference between the longer scenario and control runs, is, as already noted, associated with the warmth of the 10-year scenario run. Seasonal mean differences between the 10-year and 240-year control runs are small and nonsystematic.
- Precipitation changes calculated as the relative difference between the long scenario and control runs have much less small-scale detail than those calculated from the 10-year runs. For example, the 10-year time slice shows a pronounced south-north gradient in the change in winter precipitation between marginal decrease in southern Sweden and a 50% increase in northern Scandinavia. The difference between the 110-year scenario and 240-year control run means is in almost whole Sweden and Norway 10-20%.

Figure 24 (next page, sideways). Differences in surface air temperature (°C) between different HadCM2 runs. From left: 1) repeated scenario run – repeated control run, 2039-2049; 2) original scenario run 1990-2099 – original control run 1860-2099; 3)=(1)-(2); 4) repeated control run 2039-2049 – original control run 1860-2099; 5) repeated scenario run 2039-2049 – original scenario run 1990-2099. The first four rows show seasonal (winter, spring, summer, autumn) mean differences and the last row the annual mean. Negative values are shaded light. The darker shading in the first panel indicates the Nordic land area used in Fig. 23 and Table 7.

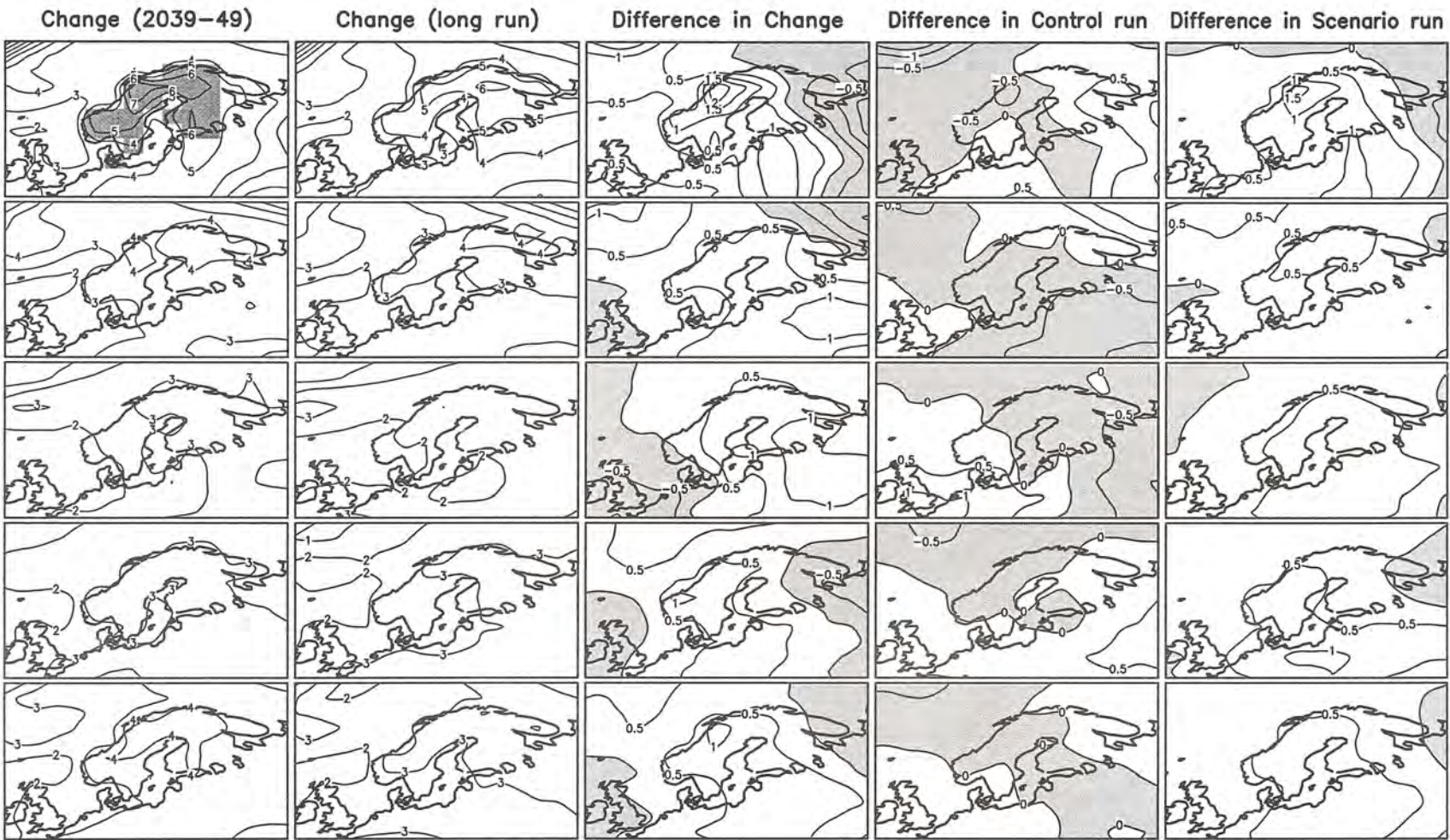
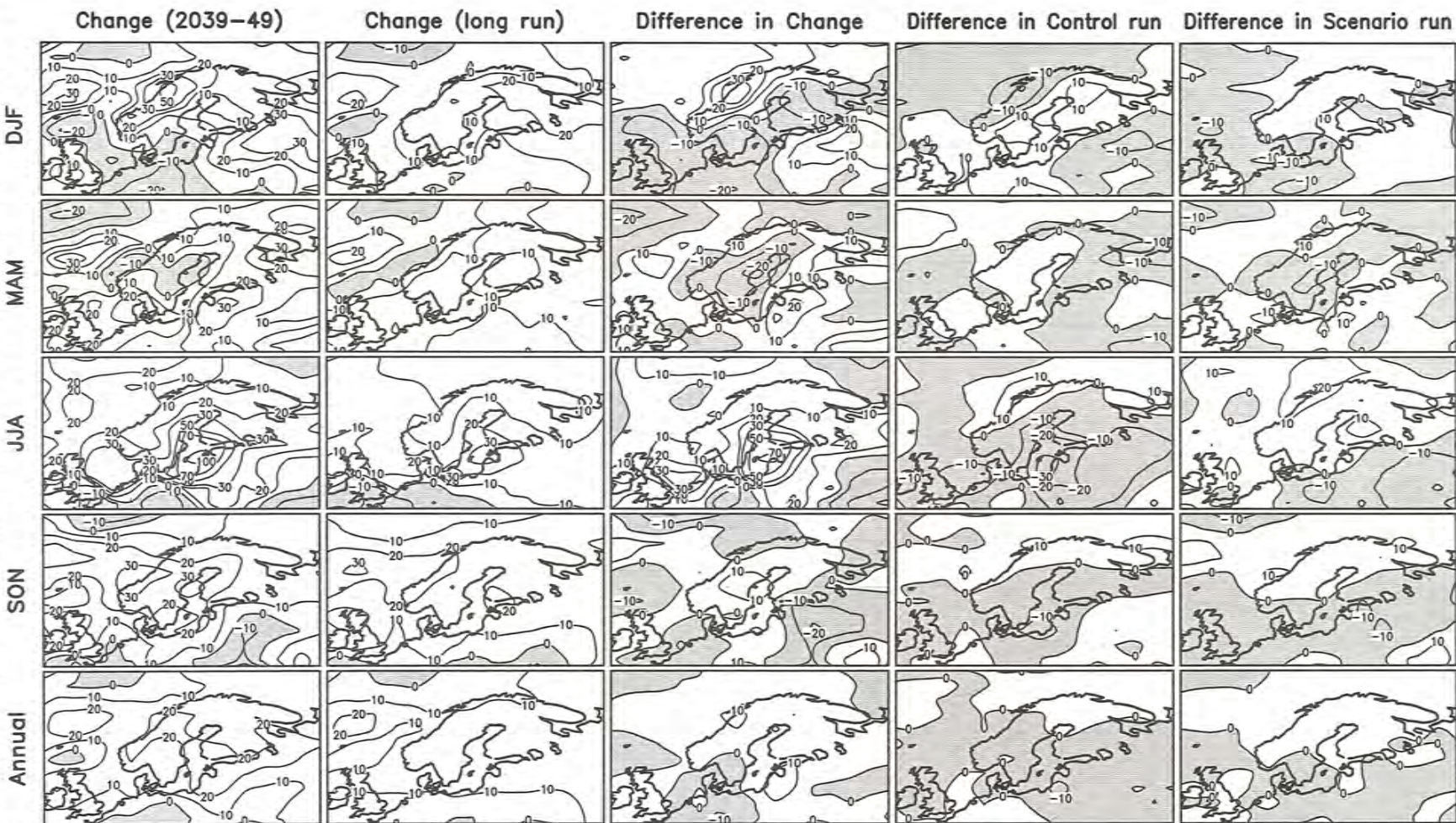


Figure 24. Caption on the previous page.

Figure 25. As Fig. 24, but differences in precipitation (%). Contours at 0, ± 10 , ± 20 , ± 30 , ± 50 , ± 70 and $\pm 100\%$



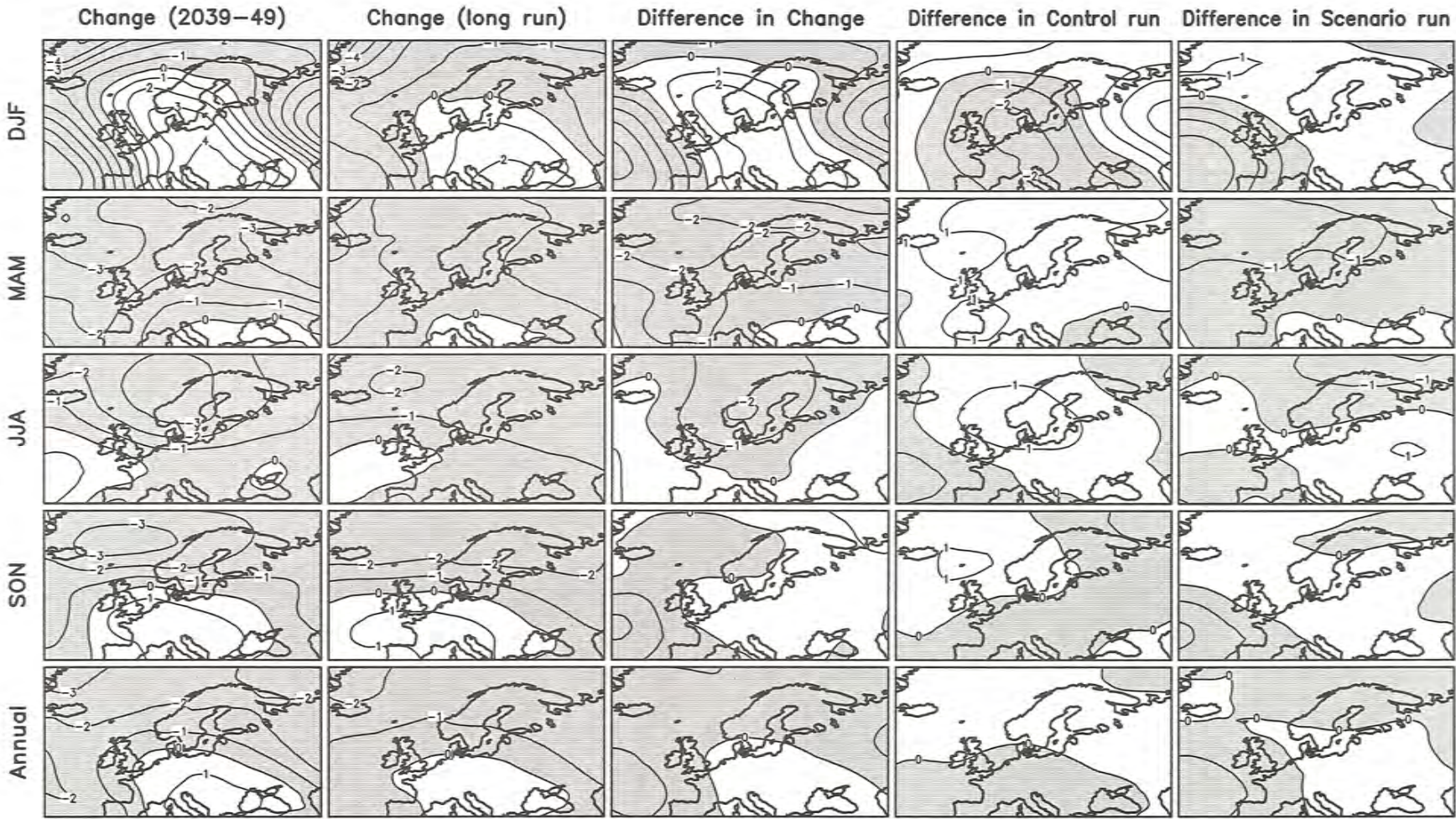


Figure 26. As Fig. 24, but differences in sea level pressure (hPa).

- A maximum increase in summer precipitation over the central Baltic Sea is present in the difference between the 110-year scenario and 240-year control runs as well, but its magnitude is much smaller (slightly over 30%) than it is in the 10-year time slice (100%). In the time slice, control run precipitation in this area is 30% below its 240-year mean, whereas scenario run precipitation is slightly above its 110-year mean. Because the change in precipitation is measured in relative units, the anomalies in the time-slice scenario and control runs add nonlinearly.
- Differences in sea level pressure between the 110-year scenario run mean and the 240-year control run mean have similarities in pattern with the difference between the 10-year scenario and control run means, but the magnitude of the long-term mean differences is smaller. This suggests that the largest pressure changes seen in the 10-year time slice occur where the truly CO₂-induced long-term change happens to be amplified by interdecadal variability. This naturally applies to many other features seen in the time slice, such as the large increase in summer precipitation over the Baltic Sea.
- The 10-year time slice indicates a more cyclonic change in summertime pressure pattern over the Nordic area than the difference between the longer scenario and control runs. The relatively large increase in summer precipitation in the time slice is consistent with this. However, it does not appear to be the case that all deviations of the time-slice (control and scenario) temperature and precipitation climates from their longer-term means would simply follow from corresponding anomalies in 10-year mean sea level pressure. In particular, the pressure differences between the 10-year and the 110-year scenario runs over northern Europe indicate only modest differences in lower tropospheric time mean winds. These differences appear insufficient to explain why the 10-year time slice is in all seasons warmer than the 110-year mean in the original scenario run.

Implicit in the discussion in this section has been that the differences between the 10-year time slice and the original, longer runs are entirely caused by interdecadal variability. This might not be literally true, since the ‘signal’ of CO₂-induced climate change in the transient scenario run could evolve nonlinearly with time. However, there is no evidence of this in the global mean surface air temperature, and nonlinearly evolving features of regional climate change are hard to separate from the strong interdecadal variability.

7 Summary and concluding remarks

The first version of the Rossby Centre regional Atmospheric climate model, RCA, and its performance in simulating present climate when driven by boundary data from a global GCM simulation were described by Rummukainen et al. (1998). The present report gives an overview of the results in the first climate change downscaling experiment made with the same model. This experiment included, in addition to the control run studied by Rummukainen et al., a scenario run representing what the climate

in northern Europe might be in a future with higher greenhouse gas concentrations. The control and scenario runs both derived their driving boundary data from global climate simulations made with the HadCM2 model (Johns et al. 1997; Mitchell and Johns 1997).

In the 10-year period used for the RCA downscaling experiment, the equivalent CO₂ concentration in the HadCM2 scenario run was 150% larger than in the control run, and the global mean surface air temperature was 2.6°C higher. Large changes were also found in the climate of northern Europe in the RCA experiment. The annual mean temperature in the Nordic region was simulated to increase by about 4°C, with largest warming in winter. This was accompanied by a substantial decrease in snow and ice cover. Precipitation was also simulated to increase in all seasons in northern Europe, in the annual mean by as much as 40% in northern Sweden. The large-scale changes in both temperature and precipitation were similar to those in HadCM2, but there were significant regional differences. For example, a dramatic decrease in ice cover in the northern Baltic Sea resulted in a sharp local maximum of wintertime warming in RCA. Because the parameterization of ice cover in this first RCA experiment was very crude, this finding is still of preliminary nature. Nevertheless, it demonstrates the importance of a proper treatment of ice-covered water bodies in simulating regional climate change in northern latitudes. In summer, on the other hand, the simulated warming was generally slightly smaller in RCA than in HadCM2.

Changes in some other climate parameters differed more markedly between RCA and HadCM2. Pronounced examples of these were total cloudiness and mean near-surface wind speed in northern Europe in winter. The RCA experiment showed a widespread decrease in wintertime cloud cover around the Baltic Sea and in much of central Europe. RCA also simulated a large increase in wintertime mean wind speed over the Baltic Sea, and a smaller but widespread increase over much of the Nordic Countries. In HadCM2, changes in both mean wind speed and total cloudiness were smaller, and the changes in total cloudiness were at times opposite to those in RCA. To some extent these differences may reflect the better ability of a higher-resolution model to describe factors important for the regional climate. For example, the increase in wintertime low-level winds in RCA over the Baltic Sea is qualitatively (although not necessarily quantitatively) consistent with reduced boundary layer stability caused by vanishing ice cover. However, different parameterizations in the global and the regional model may also be of great importance for such differences, and there is no *a priori* reason to expect that the formulations used in one model would be better than those in the other. Therefore, the existence of large differences in the response of the two models must be taken as a sign of uncertainty and as an indicator of need for further research. The decision of which model gives more plausible results can only be based on a detailed study of how realistically the relevant physical processes are represented in each of these two.

The local radiative forcing caused directly by increased CO₂ was neglected in RCA's dynamical downscaling of CO₂-induced climate change. The primary effects of increased CO₂ were assumed to be captured through advection of warmer and moister air from horizontal boundaries and through the use of HadCM2-simulated sea surface and deep soil temperatures. To a first approximation, this strategy appeared to work, since large-scale changes in temperature and precipitation in RCA and HadCM2 were similar. In the annual area mean, the warming was marginally smaller in RCA than in HadCM2 both at the surface and in the free troposphere, but it is not clear if this was primarily caused by the neglect of CO₂ increase. For example, larger surface air warming in summer in HadCM2 appeared to be explained, at least in some areas, by evaporation being more severely restricted by dryness of soil in this model. Nevertheless, the deficient CO₂ treatment appeared to have a clear signature in the top-of-atmosphere radiation balance. Outgoing long-wave radiation in the RCA scenario run was systematically larger than in the control run, which is physically unexpected and in marked contrast with the HadCM2 results. This might turn out to be a cosmetic problem that does not seriously bias the changes in surface climate, but the only rigorous way to verify this is to modify the radiation code so that the direct effect of increased CO₂ on long-wave radiation can be described.

The time mean warming in the RCA experiment was accompanied by a warming in both the lowest winter minimum temperatures and the highest summer maximum temperatures. In most of the model domain, however, the winter minima were simulated to increase more than the summer maxima. The increase in 10-year mean annual absolute minimum temperature exceeded 12°C around the coasts of the Baltic Sea and in southern and central Sweden, where, however, the crude treatment of Baltic Sea ice and low minimum temperatures in the control run complicate the interpretation. There was little systematic change in diurnal temperature variability in summer and autumn, but in winter and spring diurnal variability was simulated to decrease, especially in northern Europe. However, the quantitative results in winter are sensitive to how diurnal temperature variability is defined. Finally, considering the model domain as a whole, the mean annual number of days with precipitation remained almost constant, but days with heavy precipitation became more frequent. No evidence was found, however, that the relative increase in largest annual one-day precipitation would be much larger than the increase in total annual precipitation.

The analysis by Rummukainen et al. (1998) showed quite encouraging results; the RCA control climate was, as a whole, reasonably close to observations and in some aspects an improvement over the driving HadCM2 model. From the results of the present study, RCA also appears to be able to complement the climate change estimates given by global models with physically plausible regional detail.

One of the limitations in the present RCA experiment is its length of only 10 model years. Many of the simulated climate changes were nevertheless found to be statistically

significant against interannual variability, this being most regularly the case with surface air temperature and strongly temperature-dependent variables such as snow and ice cover. The fraction of statistically significant changes in most other parameters was also larger than what one would expect to obtain by chance, but still frequently low enough to suggest that the geographical and seasonal details of the results could be substantially changed if a longer averaging period were used. For a few variables in the HadCM2 simulation, the impact of averaging period was studied by comparing the 10-year HadCM2 runs used to drive RCA with much longer control and scenario runs made with the same model. The comparison indicated that, in the Nordic region, the difference between the 10-year scenario and control time slices in both temperature and precipitation was somewhat larger than that expected from the long-term behaviour of the HadCM2 model.

Another inevitable source of uncertainty are model deficiencies, both in the regional model and in the driving global model. The importance of having a good regional model is largest for those aspects of climate change in which the regional model is able to substantially modify the results obtained directly from the global model. Judging from the results of the first RCA experiment, such aspects include, at least, changes in cloudiness and wind conditions, and the impact of ice cover on other aspects of regional climate. To rigorously survey the uncertainty associated with the driving global model, it is clearly important to drive RCA with boundary data taken from global models other than HadCM2.

Finally, the forcing in the driving HadCM2 simulation included only an increase in equivalent CO₂ and excluded factors like sulphate aerosols and solar variability that might also affect future climate. However, if the estimates of Houghton et al. (1996) turn out to be anywhere near reality, increases in well-mixed greenhouse gases will be the single most important forcing factor in the next century. Because of the long lifetime of CO₂ and some other greenhouse gases, future changes in the greenhouse gas forcing are also more easily predictable than changes in, for example, aerosol forcing or solar variability.

Acknowledgements

The SWECLIM programme and the Rossby Centre are funded by MISTRA and by SMHI. The HadCM2 data were provided by the Hadley Centre, in part via the Climate Impacts LINK Project (Department of Environment Contract EPG 1/1/16). The testing and running of RCA has been done on the CRAY T3E at the Swedish National Supercomputing Centre (NSC) in Linköping. Several people both inside and outside the Rossby Centre made useful comments on a draft version of this report.

References

- Blondin, C., 1988: Research on land surface parameterization schemes at ECMWF. In: *Parameterization of fluxes over land surface*. Proceedings of a workshop held at ECMWF 24-26 October 1988, 285-330.
- Bringfelt, B., N. Gustafsson, P. Vilmusenaho, and S. Järvenoja, 1995: Updating of the HIRLAM physiography and climate data base. HIRLAM Technical Report No. 19, 42 pp.
- Cullen, M. J. P., and T. Davies, 1991: A conservative split explicit integration scheme with fourth order horizontal advection. *Quart. J. Roy. Meteor. Soc.*, **117**, 993-1002.
- Eerola, K., 1996: Experiences with the analysis of sea surface temperature, ice coverage and snow depth. In *HIRLAM 3 Workshop on Soil Processes and Soil/Surface Data Assimilation*, 27-29 November 1995, 33-36.
- FAO-Unesco, 1981: Soil map of the world: Vol 5, Europe. Unesco-Paris, 91 pp.
- Frei, C., C. Schär, D. Lüthi and H. C. Davies, 1998: Heavy precipitation processes in a warmer climate. *Geophys. Res. Lett.*, **25**, 1431-1434.
- Geleyn, J. F., 1987: Use of a modified Richardson for parameterizing the effect of shallow convection. *J. Meteor. Soc. Japan, Special NWP Symposium issue*, 141-149.
- Gregory, D., and S. Allen, 1991: The effect of convective scale downdraughts upon NWP and climate model simulations. 9th Conf Numerical Weather Prediction, Denver, CO, Am. Meteorol. Soc., 122-123.
- Gregory, D., and P. R. Rowntree, 1990: A mass flux convection scheme with representation of ensemble characteristics and stability dependent closure. *Mon. Wea. Rev.*, **118**, 1483-1506.
- Gustafsson, N., Ed., 1993: HIRLAM 2 final report. HIRLAM Technical Report No. 9, SMHI, Norrköping, Sweden, 126 pp.
- Houghton, J. T., L. G. Meira Filho, B. A. Callander, N. Harris, A. Kattenberg, and K. Maskell, Eds., 1996: *Climate Change 1995. The Science of Climate Change*. Cambridge University Press, 572 pp.
- Johns, T. C., 1996: A Description of the Second Hadley Centre Coupled Model (HADCM2). Hadley Centre for Climate Prediction and Research Rep. 71, 26 pp. [available from Hadley Centre, Meteorological Office, London Road, Bracknell, Berkshire RG12 2SY, United Kingdom].
- Johns, T.C., R. E. Carnell, J. F. Crossley, J. M. Gregory, J. F. B. Mitchell, C. A. Senior, S. F. B. Tett, and R. A. Wood, 1997: The second Hadley Centre coupled atmosphere-ocean GCM: Model description, spinup and validation. *Climate Dyn.*, **13**, 103-134.
- Kuo, H. L., 1965: On the formation and intensification of tropical cyclone through latent heat release by cumulus convection. *J. Atmos. Sci.*, **22**, 40-63.
- Kuo, H. L., 1974: Further studies of the parameterization of the influence of cumulus convection on large-scale flow. *J. Atmos. Sci.*, **31**, 1232-1240.

- Källén, E., Ed., 1996: HIRLAM documentation manual. System 2.5. 178 pp. + 55 pp. appendix.
- Louis, J. F., 1979: A parametric model of vertical eddy fluxes in the atmosphere. *Bound. Lay. Met.*, **17**, 187-202.
- Louis, J. F., M. Tiedtke, and J. F. Geleyn, 1981: A short history of the PBL parameterization at ECMWF, *Proc. ECMWF Workshop on Boundary-Layer Parameterization*, ECMWF, 59-79.
- Machenhauer, B., 1988: HIRLAM final report. HIRLAM Technical Report No. 5, DMI, Copenhagen, Denmark, 116 pp.
- Makin, V. and V. Perov, 1997: On the wind speed dependence of momentum, sensible heat and moisture exchange coefficients over sea in the HIRLAM model – a case study. *HIRLAM newsletter*, **29**, 26-31.
- Mesinger, F., 1981: Horizontal advection schemes on a staggered grid, an enstrophy and energy conserving model. *Mon. Wea. Rev.*, **109**, 467-478.
- Mitchell, J. F. B. and T. C. Johns, 1997: On modification of global warming by sulphate aerosols. *J. Climate*, **10**, 245-267.
- Omstedt., A and D. Cheng, 1998: Interannual variability of the maximum ice extent of the Baltic Sea and Skagerrak system in relation to large scale atmospheric circulation. *Manuscript*.
- Rummukainen, M., J. Räisänen, A. Ullerstig, B. Bringfelt, U. Hansson, P. Graham and U. Willén, 1998: RCA – Rossby Centre regional Atmospheric climate model: model description and results from the first multi-year simulation. Reports Meteorology and Climatology No. 83, SMHI, 76 pp.
- Raab, B., and H. Vedin, Eds., 1995: Climate, Lakes and Rivers. National Atlas of Sweden, vol 14, 176 pp.
- Räisänen, J., 1994: A comparison of the results of seven GCM experiments in Northern Europe. *Geophysica*, **30**, 3-30.
- Räisänen, J., 1997: Climate response to increasing CO₂ and anthropogenic sulphate aerosols – comparison between two models. Report No. 46, Department of Meteorology, University of Helsinki, 80 pp.
- Räisänen, J., 1998: Intercomparison studies of general circulation model simulations of anthropogenic climate change. Report No. 47, Department of Meteorology, University of Helsinki, 50 pp.
- Räisänen, J. and R. Döscher, 1999: Simulation of present-day climate in Northern Europe in the HadCM2 GCM. Reports Meteorology and Climatology No. 84, SMHI, 37 pp.
- Sass, B. H., L. Rontu, and P. Räisänen, 1994: HIRLAM-2 Radiation Scheme: Documentation and Tests. HIRLAM Technical Report No. 16, Norrköping, 43 pp.
- Savijärvi, H., 1990: Fast radiation parameterization schemes for mesoscale and short-range forecast models. *J. Appl. Meteor.*, **29**, 437-447.
- Seinä, A. and E. Paivosuo, 1993: The classification of the maximum annual extent of ice cover in the Baltic Sea 1720-1992 (In Finnish). *Meri*, **20**, 5-20.

- Simmons, A. J., and D. M. Burridge, 1981: An energy and angular momentum conserving vertical finite-difference scheme and hybrid vertical coordinates. *Mon. Wea. Rev.*, **109**, 758-766.
- Slingo, A., 1989: A GCM parameterization for the shortwave radiative properties of water clouds. *J. Atmos. Sci.*, **46**, 1419-1427.
- Slingo, A. and R. C. Wilderspin, 1986: Development of a revised longwave radiation scheme for an atmospheric general circulation model. *Quart. J. Roy. Meteor. Soc.*, **112**, 371-386.
- Smith, R. N. B., 1990: A scheme for predicting layer clouds and their water content in a general circulation model. *Quart. J. Roy. Meteor. Soc.*, **116**, 435-460.
- Sundqvist, H., E. Berge, and J. E. Kristjánsson, 1989: Condensation and cloud parameterization studies with a mesoscale numerical weather prediction model. *Mon. Wea. Rev.*, **117**, 1641-1657.
- Sundqvist, H., 1993: Inclusion of ice phase of hydrometeors in cloud parameterization for mesoscale and largescale models. *Beitr. Phys. Atmosph.*, **66**, 137-147.
- SWECLIM, 1998: Regional climate simulations for the Nordic region – First results from SWECLIM. SMHI, 22 pp.
- Warrilow, D. A., A. B. Sangster, and A. Slingo, 1986: Modelling of land surface processes and their influence on European climate. Met O 20 Dynamical Climatology Technical Note 38, Meteorological Office, Bracknell, UK.
- Watterson, I. G., 1997: The diurnal cycle of surface air temperature in simulated present and doubled CO₂ climates. *Climate Dyn.*, **13**, 533-545.

SMHI's publications

SMHI publishes six report series. Three of these, the R-series, are intended for international readers and are in most cases written in English. For the others the Swedish language is used.

Names of the Series

Published since

RMK (Report Meteorology and Climatology)	1974
RH (Report Hydrology)	1990
RO (Report Oceanography)	1986
METEOROLOGI	1985
HYDROLOGI	1985
OCEANOGRAFI	1985

Earlier issues published in serie RMK

- | | | | |
|---|---|----|---|
| 1 | Thompson, T., Udin, I., and Omstedt, A. (1974)
Sea surface temperatures in waters surrounding Sweden. | 8 | Eriksson, B. (1977)
Den dagliga och årliga variationen av temperatur, fuktighet och vindhastighet vid några orter i Sverige. |
| 2 | Bodin, S. (1974)
Development on an unsteady atmospheric boundary layer model. | 9 | Holmström, I., and Stokes, J. (1978)
Statistical forecasting of sea level changes in the Baltic. |
| 3 | Moen, L. (1975)
A multi-level quasi-geostrophic model for short range weather predictions. | 10 | Omstedt, A., and Sahlberg, J. (1978)
Some results from a joint Swedish-Finnish sea ice experiment, March, 1977. |
| 4 | Holmström, I. (1976)
Optimization of atmospheric models. | 11 | Haag, T. (1978)
Byggnadsindustrins väderberoende, seminarieuppsats i företagsekonomi, B-nivå. |
| 5 | Collins, W.G. (1976)
A parameterization model for calculation of vertical fluxes of momentum due to terrain induced gravity waves. | 12 | Eriksson, B. (1978)
Vegetationsperioden i Sverige beräknad från temperaturobservationer. |
| 6 | Nyberg, A. (1976)
On transport of sulphur over the North Atlantic. | 13 | Bodin, S. (1979)
En numerisk prognosmodell för det atmosfäriska gränsskiktet, grundad på den turbulenta energiekvationen. |
| 7 | Lundqvist, J.-E., and Udin, I. (1977)
Ice accretion on ships with special emphasis on Baltic conditions. | 14 | Eriksson, B. (1979)
Temperaturfluktuationer under senaste 100 åren. |

- 15 Udin, I., och Mattisson, I. (1979)
Havsis- och snöinformation ur datorbearbetade satellitdata - en modellstudie.
- 16 Eriksson, B. (1979)
Statistisk analys av nederbördsdata. Del I. Arealnederbörd.
- 17 Eriksson, B. (1980)
Statistisk analys av nederbördsdata. Del II. Frekvensanalys av månadsnederbörd.
- 18 Eriksson, B. (1980)
Årsmedelvärden (1931-60) av nederbörd, avdunstning och avrinning.
- 19 Omstedt, A. (1980)
A sensitivity analysis of steady, free floating ice.
- 20 Persson, C., och Omstedt, G. (1980)
En modell för beräkning av luftföroreningars spridning och deposition på mesoskala.
- 21 Jansson, D. (1980)
Studier av temperaturinversioner och vertikal vindskjuvning vid Sundsvall-Härnösands flygplats.
- 22 Sahlberg, J., and Törnevik, H. (1980)
A study of large scale cooling in the Bay of Bothnia.
- 23 Ericson, K., and Hårsmar, P.-O. (1980)
Boundary layer measurements at Klockrike. Oct. 1977.
- 24 Bringfelt, B. (1980)
A comparison of forest evapotranspiration determined by some independent methods.
- 25 Bodin, S., and Fredriksson, U. (1980)
Uncertainty in wind forecasting for wind power networks.
- 26 Eriksson, B. (1980)
Graddagsstatistik för Sverige.
- 27 Eriksson, B. (1981)
Statistisk analys av nederbördsdata. Del III. 200-åriga nederbördsserier.
- 28 Eriksson, B. (1981)
Den "potentiella" evapotranspirationen i Sverige.
- 29 Pershagen, H. (1981)
Maximisnödjun i Sverige (perioden 1905-70).
- 30 Lönnqvist, O. (1981)
Nederbördsstatistik med praktiska tillämpningar. (Precipitation statistics with practical applications.)
- 31 Melgarejo, J.W. (1981)
Similarity theory and resistance laws for the atmospheric boundary layer.
- 32 Liljas, E. (1981)
Analys av moln och nederbörd genom automatisk klassning av AVHRR-data.
- 33 Ericson, K. (1982)
Atmospheric boundary layer field experiment in Sweden 1980, GOTEX II, part I.
- 34 Schoeffler, P. (1982)
Dissipation, dispersion and stability of numerical schemes for advection and diffusion.
- 35 Undén, P. (1982)
The Swedish Limited Area Model. Part A. Formulation.
- 36 Bringfelt, B. (1982)
A forest evapotranspiration model using synoptic data.
- 37 Omstedt, G. (1982)
Spridning av luftförorening från skorsten i konvektiva gränsskikt.
- 38 Törnevik, H. (1982)
An aerobiological model for operational forecasts of pollen concentration in the air.
- 39 Eriksson, B. (1982)
Data rörande Sveriges temperaturklimat.
- 40 Omstedt, G. (1984)
An operational air pollution model using routine meteorological data.
- 41 Persson, C., and Funkquist, L. (1984)
Local scale plume model for nitrogen oxides. Model description.

- 42 Gollvik, S. (1984)
Estimation of orographic precipitation by dynamical interpretation of synoptic model data.
- 43 Lönnqvist, O. (1984)
Congression - A fast regression technique with a great number of functions of all predictors.
- 44 Laurin, S. (1984)
Population exposure to SO and NO_x from different sources in Stockholm.
- 45 Svensson, J. (1985)
Remote sensing of atmospheric temperature profiles by TIROS Operational Vertical Sounder.
- 46 Eriksson, B. (1986)
Nederbörds- och humiditetsklimat i Sverige under vegetationsperioden.
- 47 Taesler, R. (1986)
Köldperioden av olika längd och förekomst.
- 48 Wu Zengmao (1986)
Numerical study of lake-land breeze over Lake Vättern, Sweden.
- 49 Wu Zengmao (1986)
Numerical analysis of initialization procedure in a two-dimensional lake breeze model.
- 50 Persson, C. (1986)
Local scale plume model for nitrogen oxides. Verification.
- 51 Melgarejo, J.W. (1986)
An analytical model of the boundary layer above sloping terrain with an application to observations in Antarctica.
- 52 Bringfelt, B. (1986)
Test of a forest evapotranspiration model.
- 53 Josefsson, W. (1986)
Solar ultraviolet radiation in Sweden.
- 54 Dahlström, B. (1986)
Determination of areal precipitation for the Baltic Sea.
- 55 Persson, C. (SMHI), Rodhe, H. (MISU), De Geer, L.-E. (FOA) (1986)
The Chernobyl accident - A meteorological analysis of how radionucleides reached Sweden.
- 56 Persson, C., Robertson, L. (SMHI), Grennfelt, P., Kindbom, K., Lövblad, G., och Svanberg, P.-A. (IVL) (1987)
Luftföroreningsepisoden över södra Sverige 2 - 4 februari 1987.
- 57 Omstedt, G. (1988)
An operational air pollution model.
- 58 Alexandersson, H., Eriksson, B. (1989)
Climate fluctuations in Sweden 1860 - 1987.
- 59 Eriksson, B. (1989)
Snödjupsförhållanden i Sverige - Säsongerna 1950/51 - 1979/80.
- 60 Omstedt, G., Szegő, J. (1990)
Människors exponering för luftföroreningar.
- 61 Mueller, L., Robertson, L., Andersson, E., Gustafsson, N. (1990)
Meso- γ scale objective analysis of near surface temperature, humidity and wind, and its application in air pollution modelling.
- 62 Andersson, T., Mattisson, I. (1991)
A field test of thermometer screens.
- 63 Alexandersson, H., Gollvik, S., Mueller, L. (1991)
An energy balance model for prediction of surface temperatures.
- 64 Alexandersson, H., Dahlström, B. (1992)
Future climate in the Nordic region - survey and synthesis for the next century.
- 65 Persson, C., Langner, J., Robertson, L. (1994)
Regional spridningsmodell för Göteborgs och Bohus, Hallands och Älvsborgs län. (A mesoscale air pollution dispersion model for the Swedish west-coast region. In Swedish with captions also in English.)
- 66 Karlsson, K.-G. (1994)
Satellite-estimated cloudiness from NOAA AVHRR data in the Nordic area during 1993.

- 67 Karlsson, K-G. (1996)
Cloud classifications with the SCANDIA model.
- 68 Persson, C., Ullerstig, A. (1996)
Model calculations of dispersion of lindane over Europe. Pilot study with comparisons to measurements around the Baltic Sea and the Kattegat.
- 69 Langner, J., Persson, C., Robertson, L., and Ullerstig, A. (1996)
Air pollution Assessment Study Using the MATCH Modelling System. Application to sulfur and nitrogen compounds over Sweden 1994.
- 70 Robertson, L., Langner, J., Engardt, M. (1996)
MATCH - Meso-scale Atmospheric Transport and Chemistry modelling system.
- 71 Josefsson, W. (1996)
Five years of solar UV-radiation monitoring in Sweden.
- 72 Persson, C., Ullerstig, A., Robertson, L., Kindbom, K., Sjöberg, K. (1996)
The Swedish Precipitation Chemistry Network. Studies in network design using the MATCH modelling system and statistical methods.
- 73 Robertson, L. (1996)
Modelling of anthropogenic sulfur deposition to the African and South American continents.
- 74 Josefsson, W. (1996)
Solar UV-radiation monitoring 1996.
- 75 Häggmark, L., Ivarsson, K.-I. (SMHI), Olofsson, P.-O. (Militära vädertjänsten). (1997)
MESAN - Mesoskalig analys.
- 76 Bringfelt, B., Backström, H., Kindell, S., Omstedt, G., Persson, C., Ullerstig, A. (1997)
Calculations of PM-10 concentrations in Swedish cities- Modelling of inhalable particles
- 77 Gollvik, S. (1997)
The Teleflood project, estimation of precipitation over drainage basins.
- 78 Persson, C., Ullerstig, A. (1997)
Regional luftmiljöanalys för Västmanlands län baserad på MATCH modell-beräkningar och mätdata - Analys av 1994 års data
- 79 Josefsson, W., Karlsson, J.-E. (1997)
Measurements of total ozone 1994-1996.
- 80 Rummukainen, M. (1997)
Methods for statistical downscaling of GCM simulations.
- 81 Persson, T. (1997)
Solar irradiance modelling using satellite retrieved cloudiness - A pilot study
- 82 Langner, J., Bergström, R. (SMHI) and Pleijel, K. (IVL) (1998)
European scale modelling of sulfur, oxidized nitrogen and photochemical oxidants. Model development and evaluation for the 1994 growing season.
- 83 Rummukainen, M., Räisänen, J., Ullerstig, A., Bringfelt, B., Hansson, U., Graham, P., Willén, U. (1998)
RCA - Rossby Centre regional Atmospheric climate model: model description and results from the first multi-year simulation.
- 84 Räisänen, J., Döscher, R. (1998)
Simulation of present-day climate in Northern Europe in the HadCM2 OAGCM.



Swedish Meteorological and Hydrological Institute
SE 601 76 Norrköping, Sweden.
Tel +46 11-495 80 00. Fax +46 11-495 80 01